Bulletin of Earthquake Engineering
https://doi.org/10.1007/s10518-022-01419-7

ORIGINAL ARTICLE

Latest findings on the behaviour factor *q* for the seismic design of URM buildings

P. Morandi[1] · C. Butenweg[2] · K. Breis[3] · K. Beyer[4] · G. Magenes[1,5]

Received: 17 June 2021 / Accepted: 3 May 2022

Abstract
Recent earthquakes as the 2012 Emilia earthquake sequence showed that recently built unreinforced masonry (URM) buildings behaved much better than expected and sustained, despite the maximum PGA values ranged between 0.20–0.30 g, either minor damage or structural damage that is deemed repairable. Especially low-rise residential and commercial masonry buildings with a code-conforming seismic design and detailing behaved in general very well without substantial damages. The low damage grades of modern masonry buildings that was observed during this earthquake series highlighted again that codified design procedures based on linear analysis can be rather conservative. Although advances in simulation tools make nonlinear calculation methods more readily accessible to designers, linear analyses will still be the standard design method for years to come. The present paper aims to improve the linear seismic design method by providing a proper definition of the *q*-factor of URM buildings. These *q*-factors are derived for low-rise URM buildings with rigid diaphragms which represent recent construction practise in low to moderate seismic areas of Italy and Germany. The behaviour factor components for deformation and energy dissipation capacity and for overstrength due to the redistribution of forces are derived by means of pushover analyses. Furthermore, considerations on the behaviour factor component due to other sources of overstrength in masonry buildings are presented. As a result of the investigations, rationally based values of the behaviour factor q to be used in linear analyses in the range of 2.0–3.0 are proposed.

Keywords Unreinforced masonry buildings · Modern constructions · Seismic design · Linear elastic analysis · Behaviour factor q · Codified procedures

✉ P. Morandi
paolo.morandi@eucentre.it

[1] Department of Buildings and Infrastructures, Eucentre Foundation, Pavia, Italy

[2] SDA-Engineering GmbH, Aachen, Germany

[3] Studio Calvi, Pavia, Italy

[4] Earthquake Engineering and Structural Dynamics (EESD), School of Architectural, Civil and Environmental Engineering (ENAC), École Polytechnique Fédérale de Lausanne (EPFL), 1015 Lausanne, Switzerland

[5] Department of Civil Engineering and Architecture, University of Pavia, Pavia, Italy

Published online: 08 June 2022

1 Introduction

The realization of new load-bearing masonry buildings in European countries is far from being marginal, even in areas with considerable seismic hazard, since it is still a competitive choice for low-rise residential buildings from many points of view, not necessarily all related to seismic/structural performance, but also to excellent thermal and acoustic characteristics and fire protection.

However, in the technical and scientific community, there is still a rather common opinion that the use of structural masonry for newly designed buildings in seismic areas is "unsafe" since most collapses in recent earthquakes, e.g., in the 2009 L'Aquila (Augenti and Parisi 2010), the 2012 Emilia (Penna et al. 2014) and the 2016 Central Italy earthquakes (Sorrentino et al. 2019) occurred on loadbearing masonry structures. Suffice it to say that some extra-European structural standards (e.g., the New Zealand standard, NZS 4230, 2004) even forbid the employment of URM in seismic zones and also Eurocode 8-Part 1 (EC8-1, CEN 2005a) restricts its use, recommending for URM values of design peak ground acceleration (PGA $= a_g S$) at the ultimate limit state (ULS) not exceeding 0.20 g (return period of design action 475 years), regardless the limitation of the height of the buildings and the fulfilment of the seismic provisions.

Nevertheless, it is essential to recognize that the large majority of collapses during the past seismic events occurred to very badly detailed and badly designed (or not designed) masonry buildings (usually very low-quality old dwellings) and that, instead, the response of modern masonry buildings was found to be satisfactory up to rather large levels of seismic action. For example, the outcome of the post-earthquake inspections conducted after the 2012 Emilia earthquake sequence on modern residential and commercial masonry buildings, has shown that, in most of the cases, URM buildings sustained either minor damage or structural damage deemed repairable even in zones with estimated PGA of the events up to about 0.25–0.30 g (Penna et al. 2014; Morandi et al. 2020; Butenweg, 2013). Such satisfactory seismic behaviour was achieved on those low-rise (two- or three-storey maximum) modern masonry buildings without significant irregularities in plane and elevation, characterized by a sufficient "wall density" or number of walls in both the main directions, built with good quality materials and following the correct detailing principles.

However, the results of the safety checks adopting linear methods of analysis applied to common real structural configurations of masonry buildings using a q-factor equal to 1.5–2.0, as suggested by some seismic codes like the current version of EC8, were found to be overly conservative and in contradiction with the experimental and post-seismic evidence, whereas the results of non-linear static analyses provided results more in line with the experience, as reported in the early studies by Morandi and Magenes (Morandi 2006; Magenes 2006).

The outcomes of those researches proved that the main cause of such inconsistencies is not the definition of the level of the seismic action defined as the expected ground shaking, or the necessity of finding particular reserves of deformation or dissipation capacity in the non-linear range, but the design seismic action for the linear analysis and, therefore, the behaviour factor q.

Although non-linear static (pushover) methods provide results more in line with the actual response of the buildings and are recently more affordable for professionals thanks to some commercial software packages based on macro-modelling available in the market (e.g., among others, 2Si-PRO_SAM, 2022; Stadata-Tremuri, 2022; 3DMacro-Gruppo Sismica, 2022), it is believed that force-based linear analyses will continue to be the reference

method for the seismic design of new masonry buildings for the next years, at least in areas with moderate/medium seismic design actions. The use of linear analyses with q-factor is simple, known by practitioners and it still represents the common procedure for the seismic analysis employed in all commercial software packages for structures. Pushover procedures, whose application may require some more advanced expertise, could be instead more effective for the design of URM buildings in case of higher seismic actions or for the global assessment of old and historical masonry structures.

Therefore, driven also by the development of the new seismic codes, in particular the new Eurocode 8, following the drafting of the recently released new national norms (as the Italian and German standards), there has been an occasion to reconsider the current criteria for seismic design of masonry buildings and their consequences on practice, with particular reference to the problem of defining rationally based values of the behaviour factor q to be used in linear analyses.

In this paper, the attention is focused on a proper definition and evaluation of the q-factor of URM buildings with typical structural typologies currently being constructed in Italy and Germany constituted by low-rise (up to 3 storeys) URM buildings with in-plane rigid floors constructed in moderate seismic areas. Four-story buildings are also considered for the study of German URM, as these are typical for multi-story residential and commercial buildings. Some differences between the Italian and the German cases are present, for example in the plan configurations and construction details of the floors. Nevertheless, many of the principles developed could be suitably adapted to other typologies, following a similar rational framework. For the estimation of q-factor, pushover analyses on the different structural configurations in both countries have been performed on "global" models, since in the design of new buildings the structural conception and details imply the exploitation of in-plane strength of walls preventing any out-of-plane collapse mechanisms. Some discussion is also entrusted to the issue of the ultimate deformation limits of masonry walls to be used in the non-linear analyses. The studies of the Italian and German building configurations were executed with respect to the code concepts adopted by each country, which are implemented in the national regulations to Eurocode 6 (CEN 2005b) and Eurocode 8 (CEN 2005a).

2 The current approach for seismic design of masonry buildings and problems in linear analyses

2.1 The current approach for seismic design of masonry buildings

For the seismic design of buildings, modern codes (ASCE-FEMA 356, 2000; EC8-1, CEN 2005a; NTC 2018) consider four main methods of structural analysis: linear static (or simplified modal), linear dynamic (typically multimodal with response spectrum), nonlinear static ("pushover"), nonlinear dynamic. In the design of modern structures, the structural details (e.g., slenderness limits to the walls, connections) should prevent out-of-plane collapse and the in-plane response of walls should be checked through methods of a global analysis. Methods of global analysis that are used in common practice are essentially linear elastic (static or dynamic) or nonlinear static methods based on storey mechanism (Tomaževič 1999) or equivalent frame or macro-element idealizations (e.g., Magenes et al. 2006; Lagormarsino et al. 2013; Caliò et al. 2012).

In the linear elastic methods, using the force-based approach, the safety check procedure is usually based on at least two-level performance requirements (no collapse/severe damage and damage control); at ultimate (Severe Damage Limit State, "SDLS") the safety check consists of a strength verification, whereas for damage control ("DLS") the check is made in terms of deformation (drift) demands. The design seismic action is obtained from an elastic acceleration response spectrum scaled by a seismic force reduction factor or behaviour factor (called, hereafter, q-factor) that accounts, in an approximate way, for inelastic response at ultimate conditions. The action is applied to a linear elastic model of the structure and the resulting internal forces and displacements are calculated. In general, for masonry structures, SDLS verification is governing for DLS. The SDLS verification is carried out by checking that in each structural element the design resistance is not exceeded according to the strength criteria defined in codes. In other words, in case no redistribution of the forces is carried out, the ultimate limit state safety requirement is not met if the shear strength or the flexural strength of even just one element is exceeded. Furthermore, EC8-1 and NTC2018 also allow to implement a redistribution of the forces after linear analyses, provided that the global equilibrium is satisfied (i.e., the same base shear and position of the force resultant), the shear in any wall is reduced/increased within some limits and the consequences of the redistribution for diaphragms are taken into account.

The nonlinear static analysis (sometimes called "pushover" analysis) consists of the application to the structural model of the building of vertical gravitational loads and a horizontal force distribution that, keeping constant the relative ratio between the acting forces, is scaled to monotonically increase the horizontal displacement of a control point of the structure (e.g. the centre of the mass of the roof), up to the achievement of the ultimate conditions. The result of the nonlinear analysis is a curve (usually called "capacity curve") where the displacement of the "control point" is placed on the abscissa and the base shear is placed on the ordinates. In practice, masonry buildings can be modelled by a three-dimensional assemblage of equivalent macro-or discrete- elements where the walls, ring beams, and masonry spandrels are modelled as beam-column elements placed in the centroid of the structural members with concentrated or distributed plasticity. The walls and the horizontal elements may be characterized by an elastic–plastic behaviour with limited deformation expressed in terms of chord rotation or drift. The elements usually have linear elastic behaviour until one of the possible failure criteria (flexure or shear) is met. This idealization approximates the experimental resistance envelope under cyclic actions. More information on different non-linear modelling approaches and strategies on the seismic response of masonry structures can be found in Cattari et al. (2021).

2.2 Problems arising in linear seismic analyses of masonry buildings

Further studies have demonstrated the occurrence of some significant inconsistencies obtained from the results of the linear methods of analysis applied to common real structural configurations of masonry buildings following the standard force-based procedures (see, e.g., Butenweg et al. 2019, Morandi et al. 2020, Lagomarsino et al. 2020), confirming what found in the early works by Morandi and Magenes (Morandi 2006; Magenes 2006) and also discussed by Allen et al. (2013).

It was evident that using a q-factor equal to 1.5–2.0 as suggested by some seismic codes (e.g. the current version of EC8, CEN 2005a), it was practically impossible to satisfy strength safety checks for any configuration of two- or three storey URM buildings for PGA greater than 0.10 g. In many cases, the strength safety checks would not be satisfied

even for a_gS greater than 0.05 g. As an example, Table 1 reports the results of the linear analyses using a behaviour factor q equal to 1.5 obtained by Morandi (2006) on several simple URM buildings with rigid floors (see Fig. 1), in terms of base shear coefficient C_h ($=F/W$, where F is the base shear capacity and W is the seismic weight of the building) and maximum attainable design PGA. No redistribution of the forces was applied. The modelling of the buildings was performed considering masonry walls both coupled and uncoupled by horizontal reinforced concrete (r.c.) ring beams.

Moreover, the results of the safety checks after the elastic analyses were in contradiction with the experimental evidence and with nonlinear analyses and were thus found to be overly conservative whereas the results of nonlinear static analyses provided results more in line with the experience.

It was therefore inferred that the main cause of such inconsistencies was not the level of the seismic intensity or the necessity of finding particular reserves of deformation or dissipation capacity in the nonlinear range, but the design seismic action for elastic analysis and, therefore, the behaviour factor q. It was thus considered necessary to reconsider the criteria for the definition of the behaviour factor q.

3 Definition of the behaviour factor for seismic design of masonry buildings

The capacity of a structural system of resisting to seismic action in the non-linear range allows designing structures resorting to linear analysis with values of seismic forces smaller than those corresponding to a purely linear elastic response. In order to avoid explicit inelastic structural analysis in design, an elastic analysis can be carried out based on the use of a response spectrum reduced with respect to the elastic one by introducing the behaviour factor q. The use of the q-factor tries to take into account approximately the effects of numerous factors that concur in determining the inelastic cyclic deformation and energy dissipation capacity of a structural system. The behaviour factor q is an approximation of the ratio of the seismic forces that the structure would experience if its response was completely elastic ($F_{el,max}$) to the minimum seismic forces that may be used in the design (F_y), with a conventional elastic analysis model, still ensuring a satisfactory response of the structure (i.e. the deformation capacity is not exceeded). In the European context, important experimental references for the evaluation of behaviour factors for *URM* masonry buildings can be found in early researches carried out in Slovenia by Tomaževic et al. (Tomaževič and Weiss 1994; Tomaževič 1999; Tomaževič et al. 2004) and in Italy by Benedetti et al. (Benedetti and Castoldi 1982; Benedetti et al. 1998). With reference to Fig. 2, the response of the structure is represented by a capacity curve F-d (e.g. base shear vs. control displacement), which can be thought of as obtained from an experimental envelope curve. The typical criterion to evaluate the q-factor would be:

$$q = \frac{F_{el,max}}{F_y} \tag{1}$$

The value of F_y corresponds to the strength of an ideal bilinear system equivalent to the true nonlinear and it can be considered an estimate of the ultimate base shear capacity of the structure. Such value of strength is usually computed with energy equivalence criteria and it is slightly lower than the maximum resistance F_{max} (normally in the range between 0.90–0.95 F_{max}).

Table 1 Results of linear analyses for URM buildings (from Morandi 2006)

Structural type		*pw-X** (%)	*pw-Y** (%)	"Uncoupled" models				"Coupled" models			
				C_h		a_gS		C_h		a_gS	
				X	Y	X	Y	X	Y	X	Y
Building 1	2 storeys	3.96	5.64	*0.046*	0.145	*0.028*	0.087	*0.074*	0.158	*0.044*	0.095
	3 storeys	3.96	5.64	*0.035*	0.124	*0.025*	0.088	*0.067*	0.130	*0.047*	0.091
Building 2	2 storeys	6.05	6.19	*0.069*	0.082	*0.041*	0.049	*0.096*	0.140	*0.058*	0.084
	3 storeys	6.05	6.19	*0.044*	0.064	*0.031*	0.045	0.090	*0.074*	0.063	*0.052*
Building 3	2 storeys	3.84	3.92	0.115	*0.072*	0.069	*0.043*	0.110	*0.090*	0.066	*0.054*
	3 storeys	3.84	3.92	0.107	*0.061*	0.076	*0.043*	0.062	*0.062*	0.044	*0.044*
Building 5	2 storeys	6.34	5.54	*0.049*	0.065	*0.029*	0.039	*0.076*	0.108	*0.046*	0.065
Building 5_l.w. Y04-Y05	2 storeys	6.34	5.94	*0.060*	0.103	*0.036*	0.062	0.099	*0.095*	0.059	*0.057*
Building 5	2 storeys.[a]	6.34	5.54	*0.045*	0.057	*0.027*	0.034	0.104	*0.096*	0.062	*0.058*
Building 5_l.w. Y04-Y05	2 storeys.[a]	6.34	5.94	*0.055*	0.088	*0.033*	0.053	*0.063*	0.135	*0.038*	0.081
Building 8A	2 storeys	5.09	5.21	0.113	*0.094*	0.068	*0.056*	*0.120*	0.148	*0.072*	0.089
	3 storeys	5.09	5.21	0.091	*0.067*	0.064	*0.047*	*0.081*	0.114	*0.057*	0.080
Building 8B	2 storeys	4.43	4.14	0.114	*0.068*	0.068	*0.041*	*0.118*	0.147	*0.071*	0.088
	3 storeys	4.43	4.14	0.097	*0.054*	0.068	*0.038*	*0.080*	0.110	*0.056*	0.078
Building 8C	2 storeys	4.15	3.86	0.114	*0.067*	0.068	*0.040*	*0.110*	0.146	*0.066*	0.088
	3 storeys	4.15	3.86	0.097	*0.054*	0.068	*0.038*	*0.079*	0.110	*0.056*	0.078
Building 9	2 storeys	4.86	5.63	*0.069*	0.262	*0.041*	0.157	*0.090*	0.316	*0.054*	0.189

Italics indicate governing value of the building

*Percentage of the area of the walls relative to the floor area along X and Y, where X and Y are the main directions of the buildings. [a]Higher vertical loads

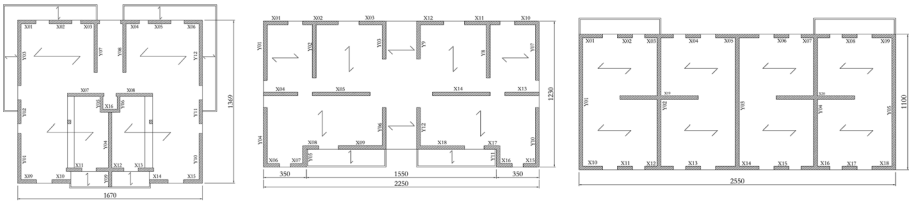

Fig. 1 Examples of plan configurations of the analysed buildings: **a** Building 1; **b** Building 8A; **c** Building 9 (Morandi 2006). All dimensions in cm

From the experimental tests carried out in the past (Benedetti and Castoldi 1982; Tomaževič and Weiss 1994; Benedetti et al. 1998; Tomaževič 1999; Tomaževič et al. 2004; Fehling et al. 2004), it was evident that the values of behaviour factor q for URM buildings well-constructed and that guarantee their "box" behaviour are in the range between 2.0 and 2.5; a strong irregularity can produce a decrease of the behaviour factor of about 30%.

This justifies the conservative choice of $q = 1.5$ that has been made by many seismic codes since the 1980s until recently (the Italian draft GNDT-CNR 1985 1985; prEC8 1–3, CEN 1995). In the current version of the EC8 (CEN 2005a), a range of q from 1.5 to 2.5 was introduced keeping however as recommended value the lower limit of the interval. Higher values of q were found in the tests on reinforced and confined masonry buildings and the values proposed in the current version of EC8 ($q = 2.0$–3.0 for confined masonry and 2.5–3.0 for reinforced masonry) appear to be in accordance with the results of the experimental tests (Tomaževič and Weiss 1994; Tomaževič 2004).

3.1 The need of the "overstrength ratio" in the definition of the *q*-factor

The first important consideration is that, according to the linear elastic analyses, the "ultimate" limit state is attained when any one wall of the building has reached its flexural or shear strength. In Fig. 2 this state is defined as F_{el} and does not correspond to the ultimate capacity of the building system.

In fact, URM elements provide a limited deformation capacity in the non-linear range that allows the building to sustain an increasing seismic load, beyond this "elastic" limit F_{el}, by increasing the forces on the other structural elements. The ultimate strength capacity (defined as F_y in Fig. 2 in the case bilinear idealization) is reached for higher values of base shear in comparison with F_{el}. Therefore, for masonry buildings, it appears evident that in the definition of the behaviour factor q it is necessary to introduce an overstrength ratio "*OSR*" ($=\alpha_u/\alpha_1$, as expressed in the current European Norms), as done for other structural typologies (r.c., steel structural systems). This factor for masonry buildings has been introduced for the first time by Morandi and Magenes (Morandi 2006; Magenes 2006), as reported in the following lines. The behaviour factor q can be therefore defined as follows:

$$q = \frac{F_{el,max}}{F_{el}} = \frac{F_{el,max}}{F_y}\frac{F_y}{F_{el}} = q^*\frac{F_y}{F_{el}} = q^* OSR \tag{2}$$

where q^* is the basic value that takes into account the deformation and dissipative capacity of the structure (equal to 1.5–2.5 for *URM* and equal to 2.5–3 for *RM* buildings according

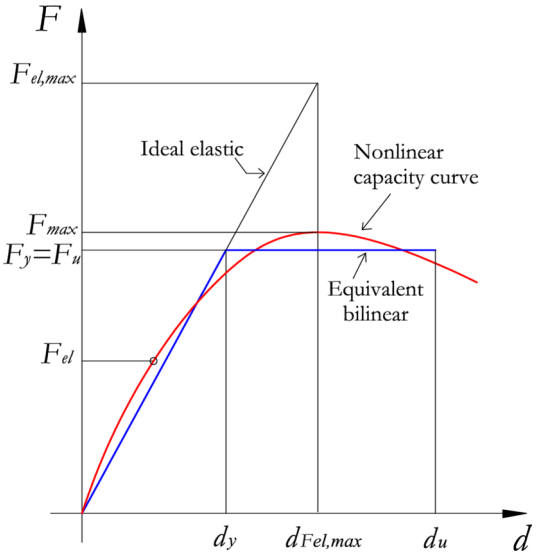

Fig. 2 Parameters for the definition of the behaviour factor q (F is the base shear, d is the displacement at a control point, e.g. the roof)

to the experimental tests) multiplied by the "overstrength ratio" $OSR = F_y/F_{el}$. Figure 3 shows the definition of q^* and OSR on the example of a typical load displacement curve with a bilinear idealisation. As it is possible to see in Fig. 3, the ultimate capacity of the buildings is reached when the structural system has attained its displacement capacity. The ultimate base shear corresponding to this point can be much higher than the base shear corresponding to the first failure, for flexure or shear, of a wall of a building. In fact, when the first failure occurs, the forces can be redistributed to the other structural elements without the structure losing any significant global resistance. Instead, the ultimate capacity of a

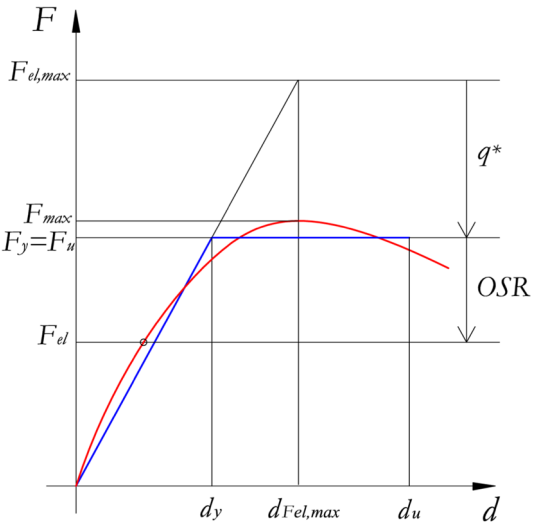

Fig. 3 Definition of the "overstrength ratio" OSR

masonry building is usually reached when the first wall of a building attains its ultimate displacement capacity.

It is expected that the *OSR* should depend, with a varying degree of sensitivity, on many factors, the most relevant ones are the following:

- Structural configuration and redundancy;
- Assumed spatial distribution (pattern) of seismic forces in elevation and in plan;
- In-plane rigidity/flexibility of diaphragms;
- Modelling assumptions regarding coupling among shear walls (flexural coupling provided by r.c. ring, beams or by masonry spandrels…);
- Modelling assumptions regarding collaboration between intersecting walls, and structural role of walls orthogonal to the seismic force;
- Modelling assumptions regarding strength criteria (e.g. shear resistance).

Because several of these factors are related to modelling hypotheses, a consistent evaluation of the "overstrength ratio" *OSR* should be performed through numerical modelling carrying out non-linear analyses.

3.2 Adopted criteria for the evaluation of *q*-factor

The values of q^* and of *OSR* ($=\alpha_u/\alpha_1$) for the evaluation of the q-factor defined previously have been estimated through the execution of a series of static non-linear analyses ("pushover") on several different structural configurations of buildings. The prototype buildings, the material properties, the structural modelling, and the results of the analyses for the evaluation of the q-factors are reported in the following sections, according to Italian and German structural configurations.

In the pushover analyses, different lateral force distributions are applied to the structures; for regular buildings these are usually:

- A force distribution proportional to the product of the masses for the deformed shape corresponding to the linear distribution of horizontal displacements along the height (sometimes called "inverse triangular-static" distribution):

$$F_j = F_{base}\frac{m_j z_j}{\sum_i (m_i z_i)} \tag{3}$$

- A force distribution proportional to the product of the masses for the deformed shape corresponding to the fundamental modal shape of vibration ("inverse triangular-modal" distribution):

$$F_j = F_{base}\frac{m_j \Phi_j}{\sum_i (m_i \Phi_i)} \tag{4}$$

- A force distribution proportional to the mass ("uniform distribution"):

$$F_j = F_{base}\frac{m_j}{\sum_i (m_i)} \tag{5}$$

where F_j is the force at *j-th* storey, F_{base} is the base shear to be applied to the structure, z_i and z_j are the heights of the storeys above the foundations, ϕ_i and ϕ_j are the displacements

of the fundamental mode shape of the *i-th* and *j-th* stories normalized in such a way that $\phi_n = 1$, where n is the control node (usually, n denotes the roof level) and m_i and m_j are the masses of the *i-th* and *j-th* stories. The analyses are carried out until the ultimate conditions of the building are exceeded, i.e., after a significant drop of the strength in the capacity curve. For each building and for each lateral force combination a nonlinear capacity curve (base shear vs horizontal displacement of the centroid of the upper floor) is obtained. For the evaluation of q^* three methods are used in this paper: the "N2 method" (Fajfar, 1999), the "modified N2 method (Guerrini et al. 2017)" and the Capacity Spectrum Method ("CSM", Freeman, 1998). The two "N2 methods" have been used for the Italian configurations, whereas the Capacity Spectrum Method for the German ones.

3.2.1 Evaluation of the over-strength ratio *OSR*

In relation to Fig. 3, the "over-strength ratio" *OSR* is estimated on the capacity curve as the ratio between the ultimate base shear of the buildings ($F_y = F_u$) and the base shear corresponding to the first failure, for flexure or shear, of a wall of a building (F_{el}). The values of F_y is evaluated with a bilinear idealization, where the elastic stiffness is found by drawing the secant of the curve in the point corresponding to 0.70 times the maximum value of the base shear, and the horizontal part of the bilinear (F_y) is found through the conservation of the areas below the effective curve and the idealized one up to the ultimate displacement of the control node in the capacity curve, corresponding to the drop of 20% of the peak (see Fig. 4b).

3.2.2 Evaluation of *q**

N2 method The first criterion employed for the evaluation of the behaviour factor q^* is based on the so-called "N2 method" (Fajfar, 1999). The method consists of reducing the MDOF capacity curve into an equivalent SDOF curve (see Fig. 4a). The SDOF model (F^*- d^*) should be determined by dividing the base shear F and top displacement d of the MDOF system with the modal participation factor Γ:

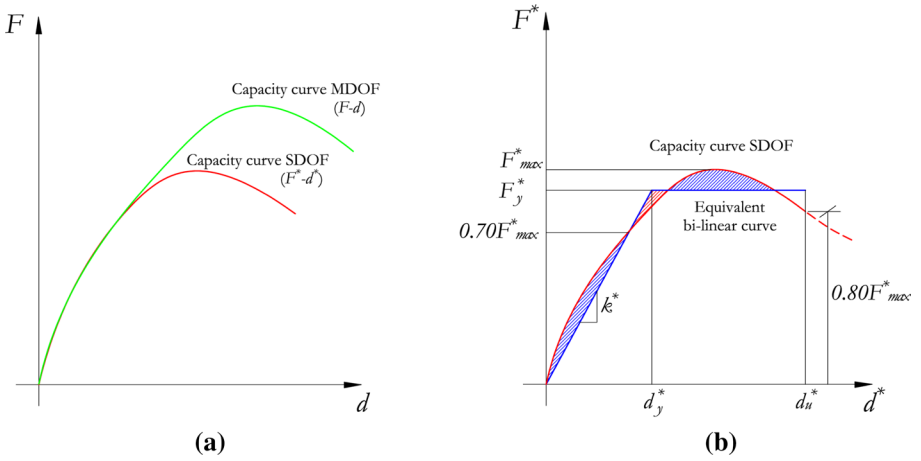

Fig. 4 **a** Force–displacement curve of the MDOF system and the SDOF system; **b** graphical procedure for the bilinear idealization of the force–displacement curve of the SDOF system

$$\Gamma = \frac{\sum_i \left(m_i \cdot_i\right)}{\sum_i \left(m_i \cdot \phi_i^2\right)} \tag{6}$$

$$d^* = \frac{d}{\Gamma} \tag{7}$$

$$F^* = \frac{F}{\Gamma} \tag{8}$$

The following step consists of the evaluation of an idealized bilinear of the SDOF capacity curve (see Fig. 4b).

The elastic period T^* and the equivalent mass m^* of the idealized system are determined as:

$$T^* = 2\pi\sqrt{\frac{m^* \cdot d_y^*}{F_y^*}} \tag{9}$$

$$m^* = \sum_i \left(m_i \cdot \phi_i\right) \tag{10}$$

where F^*_y and d^*_y are respectively the yield strength and displacement.

Once the idealized bilinear curve of the SDOF capacity curve is estimated, the inelastic displacement demand of the SDOF system d^*_{max} can be computed as:

$$d^*_{max} = \begin{cases} \frac{d^*_{e,max}}{q^*} \cdot \left[1 + (q^* - 1) \cdot \frac{T_C}{T^*}\right] \geq d^*_{e,max} \ \ if \ \ T^* < T_C \\ d^*_{e,max} \ \ if \ \ T^* \geq T_C \end{cases} \tag{11}$$

where $d^*_{e,max} = S_{De}(T^*) = (T^*)^2 S_{ae}(T^*)/4\pi^2$ is the spectral ordinate of the displacement elastic response spectrum, $S_{ae}(T^*)$ is the spectral ordinate of the acceleration elastic response spectrum at T^* and $q^* = S_{ae}(T^*) \cdot m^*/F^*_y$.

The value of q^* is calculated through the Eq. 12, derived from Eq. 11. Equations 11 are substituted in the expression for ductility $\mu = \frac{d^*_{max}}{d^*_y} = \frac{d^*_{max}}{d^*_{e,max}} q^*$, this equation is inverted, and the ductility μ is set equal to the ductility capacity $\mu_S = \frac{d^*_u}{d^*_y}$, setting $d^*_{max} = d^*_u$. The displacement capacity corresponding to ultimate limit state (d^*_u) is evaluated on the SDOF force–displacement curve as the displacement corresponding to a reduction of the force on the capacity curve by 20% of the maximum, whereas the value of the elastic yield displacement (d^*_y) is computed as the ratio between the yield strength F^*_y and the elastic stiffness of the SDOF system K_e, as shown in Fig. 4b.

$$q^* = \begin{cases} (\mu_S - 1)\frac{T^*}{T_C} + 1 \ \ if \ \ T^* < T_C \\ \mu_S \ \ if \ \ T^* \geq T_C \end{cases} \tag{12}$$

The period T_C is defined as the transition period, the border between constant acceleration and constant velocity segments of the elastic response spectrum. Type 1 and type 2

elastic response spectra $S_{ae}(T)$ of EC8 (CEN 2005a) are used, considering the five different ground types (A, B, C, D, E).

For each analysis, different values of q^* will be found according to the different elastic spectra used (due to different values of T_C).

Modified N2 method Another procedure to evaluate q^* refers to a modification of the original N2 criterion, proposed by Guerrini et al. (2017). According to the authors, such a criterion was found to be more appropriate for the evaluation of displacement demands on non-linear systems with low fundamental periods, like low-rise masonry buildings, producing slightly larger values of displacement than the original N2 method for $T < T_C$.

Once the idealized bilinear curve of the SDOF capacity curve is estimated, the inelastic displacement demand of the SDOF system d^*_{max} can be computed as:

$$d^*_{max} = \begin{cases} \frac{d^*_{e,max}}{q^*} \cdot \left[\frac{(q^*-1)^c}{\left(\frac{T^*}{T_{hyst}}+a_{hyst}\right)\left(\frac{T^*}{T_C}\right)^b} + q^* \right] \geq d^*_{e,max} \ \ if \ T^* < T_C \\ d^*_{e,max} \ \ if \ T^* \geq T_C \end{cases} \tag{13}$$

where besides the parameters already defined above, T_{hyst}, a_{hyst}, b, and c are estimated as the intermediate values of Table 2.

Then, based on the same principle reported above, the ductility μ_S is expressed as:

$$\mu_S = \begin{cases} \left[\frac{(q^*-1)^c}{\left(\frac{T^*}{T_{hyst}}+a_{hyst}\right)\left(\frac{T^*}{T_C}\right)^b} + q^* \right] \ \ if \ T^* < T_C \\ q^* \ \ if \ T^* \geq T_C \end{cases} \tag{14}$$

where $\mu_S = \frac{d^*_u}{d^*_y}$ is known from the results of the capacity curves. For $T^* \geq T_C$, q^* is simply equal to μ_S. In the case of $T^* < T_C$, since the first of the Eq. 14 cannot be explicitly inverted, the value of q^* is evaluated with an iterative procedure.

Capacity *spectrum method* The capacity spectrum method (CSM) is a nonlinear static method which compares the seismic action with the load bearing capacity of the building. The seismic action is represented by a reduced response spectrum due to damping and the building capacity is described by an inelastic pushover curve. Both curves are converted into acceleration-displacement response spectral ordinates (ADRS format). The transformation of the pushover curve into the capacity spectrum in ADRS format is carried out with an updated secant stiffness formulation to consider the damage propagation. The reduction of the response spectrum is based on the calculation of the effective damping ξ_{eff} according to Dwairi et al. 2007 and Priestley and Grant 2005 in terms of the equivalent viscous damping ξ_0 and the ductility μ:

$$\xi_{eff} = \xi_0 + c \cdot \left(\frac{\mu - 1}{\pi \cdot \mu} \right) \tag{15}$$

Table 2 Values of the parameters of the modified N2 method (Guerrini et al. 2017)

Case	a_{hyst} (–)	b (–)	c (–)	T_{hyst} (s)
Mainly FD $13\% \leq \xi_{hyst} < 15\%$	0.7	2.3	2.1	0.055
Intermediate $15\% \leq \xi_{hyst} < 18\%$	0.2	2.3	2.1	0.030
Mainly SD $18\% \leq \xi_{hyst} < 20\%$	0.0	2.3	2.1	0.022

FD Flexure dominated, *SD* Shear dominated

The constant c is applied according to Norda (2012) with 0.20 for bending failure, 0.90 for sliding and 0.44 for diagonal tension failure. These values are based on a comprehensive evaluation of cyclic shear wall tests made of typical bricks used in Germany. Furthermore, an additional damping is considered in case of bending failure due to the rocking of the wall according to Magenes and Calvi (1997), which is considered for ductility values μ greater than 1. The overall hysteretic damping of the building is calculated as the ratio of the weighted sum of the single wall damping contributions with respect to the specific failure mode:

$$\xi_{building} = \frac{\sum V_j \cdot x_j \cdot \xi_j}{\sum V_j \cdot x_j} \tag{16}$$

where V_j is the shear force, x_j is the horizontal displacement and ξ_j damping ratio of the wall j. This leads to a resulting damped spectrum with increasing damping values in the higher deformation range. Figure 5 shows the superposition of the reduced spectrum with the capacity spectrum and the "Performance Point" (PP) as intersection point of both curves (Meskouris et al. 2019).

The value of q^* is defined as the ratio of the base shear in the linear elastic and nonlinear system with the spectral accelerations $S_e(T_{el})$, $S_a(T_{PP})$ and the associated total effective masses $M_{eff,el}, M_{eff,PP}$:

$$q^* = \frac{S_a(T_{el}) \cdot M_{eff,el}}{S_a(T_{PP}) \cdot M_{eff,PP}} \tag{17}$$

where $T_{el,}$ T_{PP} and $M_{el,}$ M_{PP} are the periods associated to the initial linear elastic behaviour and the nonlinear building characteristics at the Performance Point.

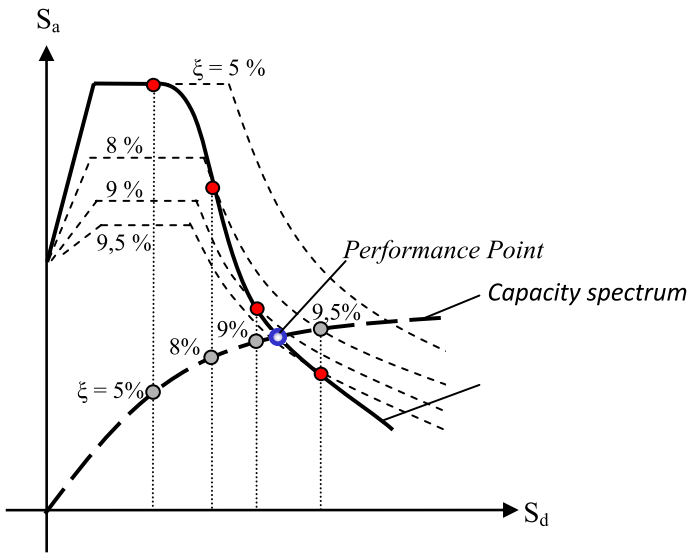

Fig. 5 Superposition of damped spectrum and capacity spectrum (Mistler et al. 2007)

3.3 Evaluation of the maximum attainable design PGA

In order to estimate the maximum seismic performance of the analysed buildings, the maximum attainable design PGA (a_gS) values is calculated by means of the N2, the modified N2 and the CSM method.

For the N2 and modified N2 method, the maximum attainable design PGA is derived by assuming the displacement demand to be equal to the displacement capacity of the building, d_u:

$$d^*_{max} = \frac{d_u}{\Gamma} \tag{18}$$

In the case of N2 method, the inelastic displacement demand of the SDOF system d^*_{max} is calculated as reported in the Eq. 11, whereas, in the case of the modified N2 method, the displacement d^*_{max} is computed according to the expressions (14). In both cases, q^* cannot exceed the value of 3, according to a requirement in the Italian norms that serves as a limitation of the maximum ductility of the system. Knowing all the other parameters, it is possible to evaluate $d^*_{e,max}$ and therefore the spectral ordinate of the displacement response spectrum at T^* ($S_{De}(T^*)$). Finally, given the characteristics of the spectra, it is possible to calculate the corresponding values of the attainable design PGA (a_gS).

For CSM method, the maximum attainable design PGA is calculated in an iterative procedure by scaling up the PGA as long as a Performance Point can be evaluated before the horizontal resistance drops down to less than 80%.

4 Evaluation of the *q*-factor in past experiences and indications in the Italian and German seismic codes

4.1 Italian experience

In Italy, two main numerical studies were performed in the past to evaluate the q-factor in line with the assumptions reported above.

The first investigation was carried out by Morandi and Magenes (Morandi 2006; Magenes 2006) on one, two, and three-storey URM masonry buildings (4 single-storey and 19 two/three-storey prototypes) with structural configurations typical of the Italian construction techniques, having continuous r.c. ring beams at the level of each floor/roof and rigid diaphragms (see example in Fig. 1). Table 3 summarizes the parameters used in the analyses. Strength criteria for flexure and shear were adopted as those in the equations of Table 9. The modelling assumptions are the same of those illustrated in Sect. 5.2 considering and not considering the coupling effects of the r.c. ring beams. The values of *OSR* were computed as reported in Sect. 3.2.1 through the execution of pushover analyses on the building configurations with the aid of the software SAMII (Magenes et al. 2006); the value of q^* was fixed as 2.0 for regular and 1.5 for irregular buildings, as suggested by the results of dynamic tests on scaled prototypes (Tomaževič and Weiss 1994; Tomaževič 2004; Benedetti and Castoldi 1982; Benedetti et al. 1998; Benedetti 2004). Elastic spectra of the Italian norm OPCM3274 (2003) were adopted. In the case of flexural response the ultimate deformation capacity of masonry

Table 3 Strength and stiffness parameters used in the analyses

	Characteristic values	Mean values*
Compressive strength of masonry f (MPa)	4.50	6.43
Cohesion of masonry f_{v0} (MPa)	0.20	0.28
Shear strength limit of masonry f_{vlim} (MPa)	1.50	2.20
Elastic modulus of masonry E (MPa)	4500	
Elastic modulus of masonry G (MPa)	1800	
α, cracking coefficient of masonry [-]	0.50	
Compressive strength of concrete on cylinder f_c (MPa)	20	28
Yield strength of reinforcing steel f_y (MPa)	430	467
Elastic modulus of concrete E_c (MPa)	28,500	
Shear modulus of concrete G_c (MPa)	11,400	
α, cracking coefficient of concrete (–)	0.50	

*Parameters used in pushover analyses

walls was imposed equal to 0.8%, whereas, in the case of shear response equal to 0.40%, being the reference ultimate drift limits assumed for URM walls in that period.

The results of the overstrength ratio (*OSR*) on two- and three-storey URM buildings (19 along X and 19 along Y direction) are reported in Fig. 6 for both the flexural coupled (a) and uncoupled models (b). The values of *OSR* for flexural coupled single storey buildings are slightly lower (from 1.40 to 2.15).

The range of variation of *OSR* is extremely wide. However, in the case of flexural coupled two/three-storey systems, all the buildings have, at least in one of the main directions (X or Y), an *OSR* higher than 2.0. The minimum value of *OSR* belongs to a building made up by parallel walls of about the same directions and without any opening ("terraced house", building 9 of Fig. 1c) and therefore similar to parallel non-coupled cantilevers for which an overstrength ratio close to 1.0 is expected (Magenes and Morandi 2008).

Based on such results, the update of the Italian norms (OPCM 3431 2005) was the first code to introduce a new definition of q-factors for masonry buildings, as the product between q^*, i.e., the basic value that takes into account the deformation/dissipation

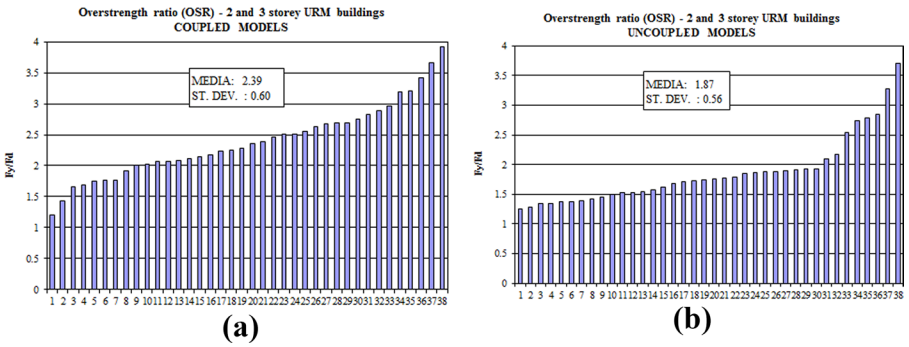

Fig. 6 Calculated *OSR* values for 2 and 3 storey URM buildings **a** On flexural coupled model and **b** On flexural uncoupled model (Morandi 2006; Magenes 2006)

Table 4 Strength and stiffness parameters used in the analyses (mean values)

	F	MP	TG
Compressive strength of masonry f (MPa)	9.50	5.34	5.30
Cohesion of masonry f_{v0} (MPa)	0.23	0.54	0.115**
Shear strength limit of masonry f_{vlim} (MPa)	2.20	2.20	2.20
Elastic modulus of masonry E (MPa)	5900	4200	3874
Elastic modulus of masonry G (MPa)	1800	1680	1550
α, cracking coefficient of masonry (–)	0.30	0.40	0.28
Compressive strength of concrete on cylinder f_c (MPa)	28	28	28
Yield strength of reinforcing steel f_y (MPa)	467	467	467
Elastic modulus of concrete E_c (MPa)	30,000	30,000	30,000
Shear modulus of concrete G_c (MPa)	12,500	12,500	12,500
α, cracking coefficient of concrete (–)	0.50	0.50	0.50

**For masonry with perpend joints unfilled, the value of f_{v0} has been found by halving the value of the gross cohesion in accordance with the EC6 requirements

capacity of the structure (assumed equal to 2 for regular and 1.5 for non-regular buildings) and the "overstrength ratio" *OSR*:

- URM building, regular in elevation, $q = q^* \cdot OSR = 2.0 \cdot OSR$
- URM building, non-regular in elevation, $q = q^* \cdot OSR = 1.5 \cdot OSR$

with the values of *OSR* equal to:

- Single storey URM buildings, $OSR = 1.4$
- Two or more storey URM buildings, $OSR = 1.8$

In the case of multi-storey URM buildings regular in elevation the value of q could be taken as $2.0 \cdot OSR = 2 \cdot 1.8 = 3.6$. The further update of the Italian norms in 2008 (NTC 2008) maintained unchanged these values.

The second numerical investigation was carried out a few years later, when an in-deep revision of the drift capacity for shear failure provided by new available experimental results on URM piers revealed that the limit of 0.4% was unconservative, above all on modern masonry typologies (Magenes et al. 2008). Therefore, a new numerical campaign was performed on one, two and three-storey structural configurations (2 single storey-, 8 two storey- and 6 three storey-prototypes) similar to those considered in the research by Morandi in 2006 (Frumento et al. 2009). Flexural and shear strength criteria as those in equations of Table 9 were adopted. The modelling assumptions were the same as those illustrated in Sect. 5.2, considering the coupling effects of the r.c. ring beams and rigid diaphragms. For the evaluation of q^* the "N2 method" was used and for the computation of OSR the criterion in Sect. 3.2.1 was employed, through the execution of pushover analyses using the software SAMII. Also, in this case, the elastic spectra were those of the Italian norm OPCM3274. Modern masonry typologies with the characteristics reported in Table 4 were adopted: "traditional" masonry with a general-purpose mortar and fully grouted head-joints (called "F"), masonry with units with a pocket filled with mortar ("MP") and masonry with dry head-joint and tongue and groove units ("TG"). In the case of flexural

Table 5 Values of the minimum and mean values of q^*, *OSR*, and q (Frumento et al. 2009)

	"F"–$\theta_{u,shear}$ = 0.25%				"MP"–$\theta_{u,shear}$ = 0.25%				"TG"–$\theta_{u,shear}$ = 0.21%			
	1 storey		2–3 storeys		1 storey		2–3 storeys		1 storey		2–3 storeys	
	Min	Mean	Min	Mean	Min	Mean	Min	Mean	Min	Mean	Min	Mean
q^*	2.20	2.70	1.70	2.30	2.20	5.20	1.70	3.30	2.10	2.30	1.50	1.80
OSR	1.60	2.30	1.70	2.40	1.90	2.50	1.70	2.90	1.30	2.00	1.50	2.40
q	4.20	–	3.00	–	5.30	–	3.70	–	3.00	–	2.50	–

response, the ultimate deformation capacity of masonry walls was imposed equal to 0.8%, whereas in the case of shear response equal to 0.25% for "F" and "MP" and to 0.21% for "TG". Such input data were derived from an interpretation of a dataset of in-plane cyclic tests (see Frumento et al. 2009).

The results of q^*, *OSR* and q are reported in Table 5.

For the three main typologies of URM considered ("F", "MP" and "TG"), conservative values of q for design were proposed as 3.00 for F and MP masonry and 2.50 for TG masonry, in the case of buildings regular in elevation. Such values are a result of the ductility and the overstrength ratio (*OSR*) of the structural systems. The lower factor of 2.50 for TG masonry is a consequence of the lower ultimate displacement capacity found in the experiments for the case of shear failures.

The results of this research have provided the background for the evaluation of the behaviour factor in the recently released 2018 Italian Norms (NTC2018), where the value of q-factor for URM buildings regular in plan and elevation was set to $q^* \cdot OSR = 1.75 \cdot 1.70 = 2.975$. In the case of buildings non-regular in elevation, the q-factor needs to be reduced by 0.80, whereas in case of a building non-regular in plan *OSR* should be decreased to 1.35. The Italian Norms currently forbid the use of masonry with unfilled head-joints unless in areas with low seismicity.

4.2 German experience

In Germany, early experimental investigations for the evaluation of increased behaviour factors for URM masonry walls with respect to the geometry and vertical load level were carried out by Fehling et al. (2004). The seismic design situation for representative URM buildings in Germany has been analysed within the research project ISEDEM (Butenweg et al. 2019) considering the new German hazard maps. The first step of the project was the analyses of 28 representative URM buildings in German earthquake regions (Fig. 7a) using the traditional force-based design concept with uncoupled flexural modelling and a behaviour factor of 1.5. By using these assumptions, it was only possible to verify traditional building configurations in transitions zones close to very low seismicity. Therefore, more realistic modelling assumptions and q-factors have been developed and introduced in the new seismic design code. The improvement of the new design rules is shown on the example of the URM building 05-MFH-CB-2. Figure 7 shows the areas with successful verification in green colour for the traditional approach (Fig. 7a), the approach with increased q-factors (Fig. 7b) and pushover analyses (Fig. 7c). Considering the experiences of past earthquakes, the results with increased q-factors and pushover analyses are much

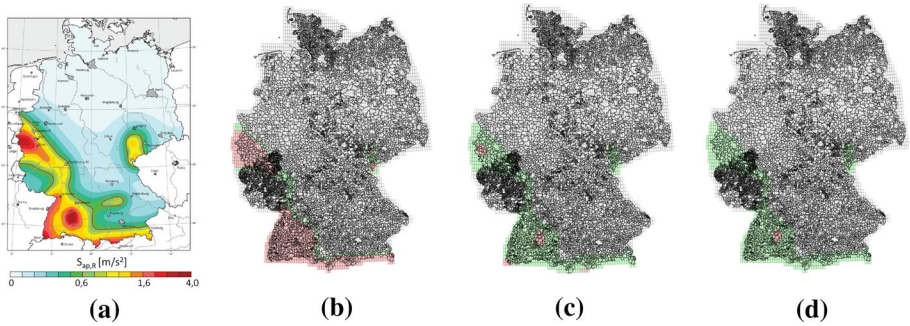

Fig. 7 **a** German hazard map with maximum spectral accelerations $S_{ap,R}$ on rock, **b** Linear verification results with $q = 1.5$ and uncoupled flexural modelling **c** Verification results with $q = 2.4$ and flexural coupled modelling and **d** Verification using nonlinear calculations

more realistic for values of PGA in German earthquake regions ranging between 0.05 g to 0.16 g.

If not evaluated through pushover analysis the q-factor should be estimated in each design direction as follows:

$$\frac{h}{l} \leq 1 : q = 1.7\frac{\alpha_u}{\alpha_1} \text{and} \frac{h}{l} \geq 1.6 : q = 2.0\frac{\alpha_u}{\alpha_1} \tag{19}$$

The overstrength factor α_u/α_1 can be applied with 1.15 and the axial load ratio σ_0/f_k should not exceed 15%, if q^* exceeds 1.7. The q-factor can be increased up to 2.7 if the choice of a higher overstrength factor α_u/α_1 and/or q^* is justified through pushover analysis. The seismic code renounces further regulations, such as the required number of walls in the principal building directions, and leaves the final choice of higher values to the practising engineer. In comparison to the former code version, the q-factor is increased by a factor in the range 1.33–1.80, which will allow much better a successful verification of low-rise masonry buildings with proper seismic design and detailing in German earthquake regions with low to moderate seismicity.

5 Evaluation of the *q*-factor for "Italian" structural configurations

5.1 Structural configurations and material properties

Six different configurations of URM buildings with one to three storeys with a wall thickness equal to 240, 300, 350, and 400 mm have been considered (total of 72 prototype buildings). They are characterized by a rather simple configuration in plan and regularity in elevation, with a total area of shear walls ranging between about 3.2% and 8.6% of the total floor area in each principal direction (see Figs. 8 and 9).

The clear inter-storey height in all buildings is 2.85 m and the height of the openings is equal to the inter-storey height, assuming the absence of structurally effective masonry parapets and spandrels. The floor slabs, realized with r.c. joists and clay tiles with a 50-mm-thick r.c. topping (total thickness of 250 mm), are considered to have a rigid in-plane diaphragm behaviour. At each floor level, all walls are connected by continuous r.c. ring beams, which are assumed to have a width equal to the wall thickness

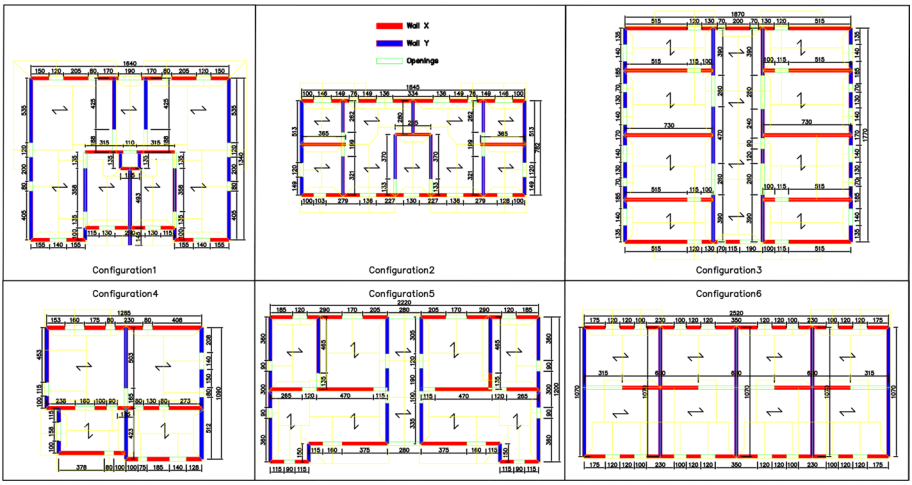

Fig. 8 Structural configurations in plan

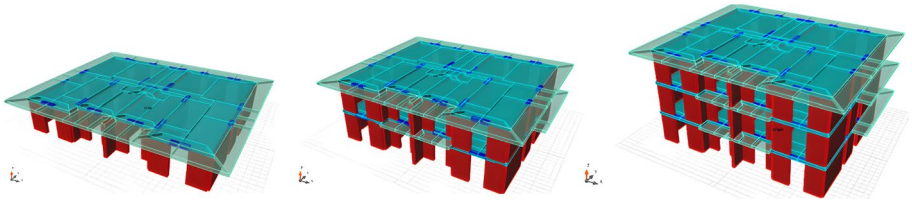

Fig. 9 3D view of configuration 1 with one, two and three storeys

and a height equal to the floor height. The ring beams are reinforced with 4 ϕ 16 mm rebars (2 at the top and 2 at the bottom, $401 + 401$ mm^2) and ϕ 6 mm 2 leg closed stirrups at 250 mm spacing, corresponding to the minimum reinforcement required in the Italian national provisions.

In Table 6 the structural configurations of all the buildings, the values of the percentage of the area of the walls relative to the floor area along X and Y (*pw-X*, *pw-Y*) and the seismic weight (*W*) of all the structures, calculated with the exclusion of the self-weight of half-height of the base walls, are reported.

The mechanical properties used in analyses are typical of modern masonry constructions in Italy, with fully filled general-purpose mortar head-and bed-joints. In order to estimate the properties of the masonry, the use of low values compressive strength of the units and mortar has been assumed, according to the recommended minimum values of the current EC8. Starting from these values, the characteristic values of the masonry parameters have been obtained according to NTC2018 and Eurocode 6 (CEN 2005b). Table 7 summarizes the parameters used in the analyses, where the mean values of the strength, to be used in pushover analyses, have been computed dividing the characteristic values by 0.80, consistently with the standards for masonry characterization tests. Finally, factor α, that takes into account the cracked shear and flexural elastic stiffness of the masonry walls, is set equal to 0.50, in line with the indications of NTC2018 and EC8.

Table 6 Structural configurations, wall thicknesses, percentage of walls and total weight

Structural configurations	Wall thickness (mm)	pw-X (%)	pw-Y (%)	W 1 st. build. (kN)	W 2 st. build. (kN)	W 3 st. build.(kN)
Configuration 1	240	3.20	5.31	2396	4777	7159
	300	3.97	6.56	2464	4980	7496
	350	4.60	7.57	2520	5148	7777
	400	5.22	8.56	2576	5317	8058
Configuration 2	240	5.32	5.47	1760	3495	5229
	300	6.58	6.74	1819	3671	5523
	350	7.59	7.76	1868	3818	5768
	400	8.59	8.75	1917	3965	6013
Configuration 3	240	4.69	3.17	3461	6688	9907
	300	5.81	3.93	3558	6978	10,390
	350	6.71	4.56	3639	7220	10,793
	400	7.60	5.17	3719	7461	11,195
Configuration 4	240	4.65	4.36	1628	3073	4517
	300	5.75	5.38	1674	3208	4743
	350	6.64	6.21	1711	3321	4931
	400	7.51	7.01	1749	3434	5119
Configuration 5	240	4.05	4.68	2722	5170	7619
	300	5.02	5.80	2800	5406	8012
	350	5.81	6.71	2866	5603	8340
	400	6.58	7.61	2931	5800	8668
Configuration 6	240	3.91	4.55	2950	5618	8285
	300	4.86	5.63	3035	5871	8708
	350	5.63	6.50	3105	6083	9060
	400	6.39	7.36	3176	6294	9413

Table 7 Strength and stiffness parameters used in the analyses

	Characteristic values	Mean values*
Compressive strength of unit f_b (MPa)	5.00	6.00 (normalized)
Compressive strength of mortar f_m (MPa)	–	5.00
Compressive strength of masonry f (MPa)	3.30	4.125
Cohesion of masonry f_{v0} (MPa)	0.20	0.25
Shear strength of masonry limit f_{vlim} (MPa)	$(=0.065f_{b,norm})$ 0.39	$(=0.065/0.8f_{b,norm})$ 0.49
Elastic modulus of masonry E (MPa)	3300	
Elastic modulus of masonry G (MPa)	1320	
α, cracking coefficient of masonry (–)	0.50	
Compressive strength of concrete on cylinder f_c (MPa)	20	28
Yield strength of reinforcing steel f_y (MPa)	450	475
Elastic modulus of concrete E_c (MPa)	30,200	
Shear modulus of concrete G_c (MPa)	12,584	
α, cracking coefficient of concrete (–)	0.50	

*Parameters used in pushover analyses

Table 8 Gravity loads of the analysed buildings

	Floor load	Roof load	Staircase and balcony
Slab system self-weight, g_{k1} (kN/m^2)	3.00	6.00*	5.00
Permanent actions, g_{k2} (kN/m^2)	3.00	1.50	1.00
Variable actions, q_k (kN/m^2)	2.00	1.20** (snow)	4.00

*Sum of the horizontal floor under the roof and the roof pitch; ** the load is zero in the seismic combination of actions

Table 9 Strength criteria and ultimate deformation capacities

	Resistance	Ultimate deformation θ_u
Bending and axial force	$M_{Rd} = \frac{l^2 \cdot t \cdot \sigma_0}{2} \cdot \left(1 - \frac{\sigma_0}{0.85 \cdot f_d}\right)$	0.80%
Shear:	$V_{Rd} = f_{vd} l' t$ with $f_{vd} = \min\left(f_{vd1}; f_{vd2}\right)$ $f_{vd1} = f_{v0} + 0,4 \cdot \sigma_d$ $f_{vd2} = f_{vlim} = \frac{0.065}{0.80} f_b$	0.20%; 0.25%; 0.30%;0.40%

l, h, t: length, height and thickness of the wall; $f_d = f$: mean value of the compression strength of the masonry; σ_v and σ_d: respectively, compression stress on the gross section ($\sigma_0 = N/(t \cdot l)$) and on the portion of the wall in compression ($\sigma_d = N/(t \cdot l')$, *N*: vertical load of the wall; *l'* compressed part of the section; f_{v0} mean value of the initial shear strength; f_b: normalized vertical compression strength of the units

A coefficient equal to 1/0.8 = 1.25 has been applied to obtain a "mean" value of f_{vlim} from the characteristic value of f_{vklim}, in accordance with EN 1052–3 that recommends a value of 0.80 between the mean and characteristic shear strength

The vertical loads used in the analysed buildings are reported in Table 8. The vertical loads and the masses have been calculated with the "seismic" combination of the gravity loads in accordance with Eurocode 0 (CEN 2002) and Italian NTC (2018). The specific weight of the masonry has been assumed equal to 10 kN/m^3 (perforated units).

5.2 Modelling approach and execution of pushover analyses

The model is conceived for the global analysis of masonry buildings where the resisting mechanism is governed by in-plane response of walls. Collapse mechanisms due to out-of-plane response are not considered in the model, assuming that are inhibited for the employment of suitable details.

The masonry buildings are modelled by a three-dimensional equivalent frame with walls and ring beams modelled as beam-column elements placed in the centroid of the structural elements and constituted by a deformable part and rigid ends. It is assumed that intersecting walls are effectively bonded together, as in typical Italian constructions, and the bond is modelled through "rigid links" maintaining the continuity of vertical displacements at the corners at the level of the floor level ("flexural coupled modelling", see Fig. 10a). A second modelling option is also provided, and it is characterized by the absence of any horizontal element ("flexural uncoupled modelling", see Fig. 10b); this case can allow extending the results also to configurations without coupling horizontal elements (without r.c. ring beams

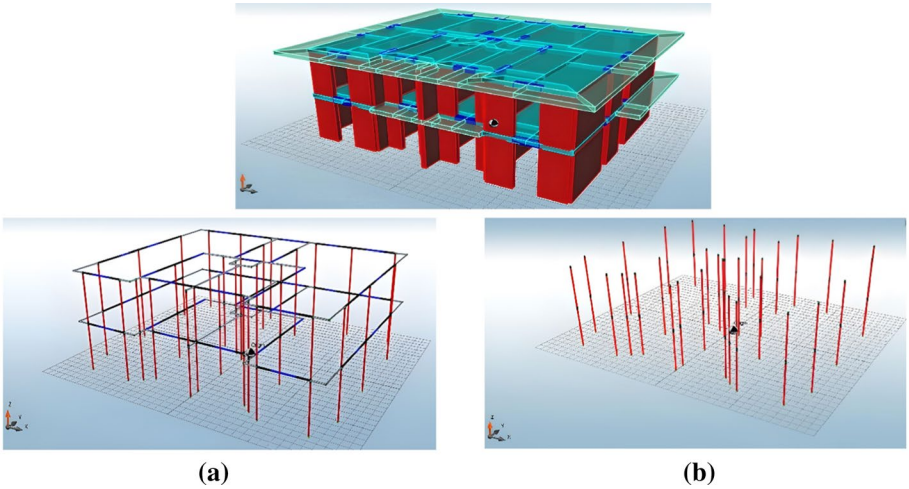

Fig. 10 **a** "Flexural coupled" and **b** "flexural uncoupled" modelling approach

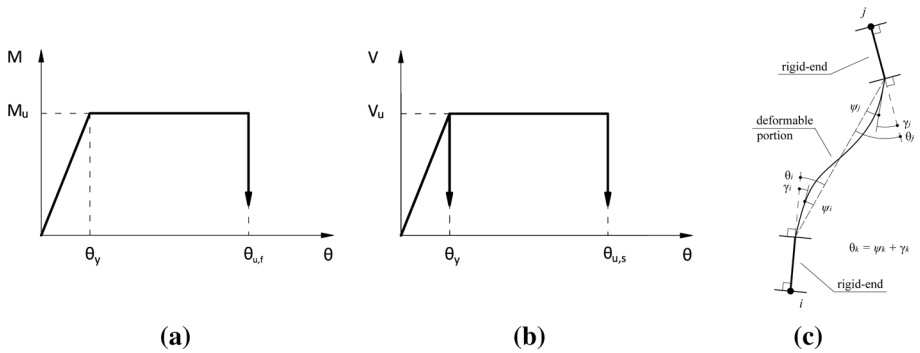

Fig. 11 Elastic–plastic behaviour of masonry walls: **a** Flexural response; **b** Shear response; **c** chord rotation in a wall-beam element

but, for example, with steel ties which are flexurally ineffective), typical of the construction practice in some non-Italian countries.

The walls and the horizontal elements are supposed to have an elastic–plastic behaviour with limited deformation. The elements have a linear elastic behaviour until one of the two possible failure criteria, for flexure or shear, is met. This idealization approximates the experimental resistance envelope under cyclic actions. The flexural failure occurs when the bending moment in one of the two end sections reaches the ultimate flexural resistance M_{Rd}, whereas the shear failure occurs when the shear in one of the two end sections reaches the ultimate shear resistance V_{Rd}. The expression for M_{Rd} is based on the common ultimate flexural resistance of URM masonry elements, whereas the formulation for V_{Rd} is taken as recommended in NTC2018 and EC6, which represents typical shear failures in modern block masonry; such expressions are summarized in Table 9. The failure criteria are formulated in such a way that, if the vertical load in the URM walls is zero, both the shear and flexure resistance are also null.

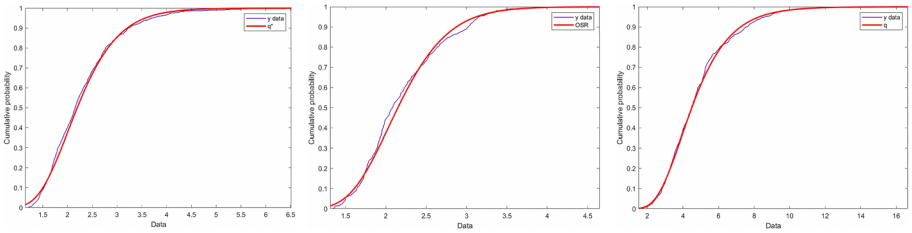

Fig. 12 Distribution of q^* **a**, *OSR* **b** and q **c** for the case of equivalent frame modelling, modified N2 method and $\theta_{u,shear} = 0.30\%$

When the failure criteria are met, plastic deformations occur as illustrated in Fig. 11a for flexural response and in Fig. 11b for shear response, where a limit θ_u to the maximum chord rotation is set, beyond which the strength and the stiffness of the wall are zeroed. The chord rotation is expressed as the sum of the flexural deformation and the shear deformation as a generalization of the concept of drift for non-symmetric boundary conditions of a pier subjected to flexure and shear (see Fig. 11c).

In the case of flexural response, the ultimate deformation capacity of masonry walls has been imposed equal to 0.8% whereas, in the case of shear response, four different values have been used: 0.20%, 0.25, 0.30 and 0.40% (see Table 9) and four different batches of analyses have been carried out. The motivation for the choice of these drift values is reported in Sect. 7.1. For the selected structural configurations, the limit governing the design has always resulted to be the deformation capacity in shear. R.c. ring beams have been modelled with an elastic perfectly plastic behaviour with flexural and shear failure and consequent formation of plastic hinges. The flexural and the shear strength of the ring beams were computed with the traditional formulations used for reinforced concrete. All the pushover analyses have been carried out using software PRO_Sam (2Si) based on the solver SAM II.

5.3 Results of the analyses: *q*-factor and attainable design PGA

On each of the 72 building prototypes (6 plan configurations × 4 different wall thicknesses × 3 storeys), 24 pushover analyses have been carried out (X/Y directions, ± loadings, ± accidental eccentricities, "inverse triangular-static"/ "inverse triangular-modal"/"uniform" lateral distributions). For each building prototype and for each direction, the minimum of the 12 values of the system ductility μ_S and *OSR* has been considered, in order to have a single value of these two parameters along X and along Y.

Then, for the evaluation of the basic values of q^*, the N2 method and modified N2 method have been used, as illustrated in Sect. 3.2. Both methods need the evaluation of the spectral accelerations, which are provided with reference to type 1 and type 2 response spectra of the current version of EC8 with 5 soil categories.

Therefore, a total of 144 values of *OSR* have been obtained and, for each method, 1440 values of q* and q. The values of the 5th, 10th, and 50th percentile have been calculated, with a fit using a lognormal distribution (an example is shown in Fig. 12). In Tables 10 and 11, the values of the 5th, 10th and 50th percentile of *OSR*, q^* and q are reported, subdivided according to each method, with or without horizontal coupling elements and as

Table 10 Values of the 5th, 10th and 50th percentiles of q^*, *OSR* and q–buildings with 1, 2 and 3 storeys, "flexural coupled" modelling

Percentile	$\theta_{u,shear}=0.20\%$			$\theta_{u,shear}=0.25\%$			$\theta_{u,shear}=0.30\%$			$\theta_{u,shear}=0.40\%$		
	5%	10%	50%	5%	10%	50%	5%	10%	50%	5%	10%	50%
N2 method												
q^*	1.23	1.39	2.11	1.35	1.53	2.42	1.45	1.67	2.71	1.69	1.96	3.33
OSR	1.43	1.56	2.08	1.46	1.58	2.11	1.49	1.61	2.16	1.51	1.63	2.16
q	2.19	2.53	4.21	2.43	2.85	4.92	2.71	3.17	5.58	3.11	3.71	6.88
Modified N2 method												
q^*	1.26	1.38	1.89	1.32	1.45	2.05	1.36	1.51	2.20	1.38	1.54	2.26
OSR	1.43	1.56	2.08	1.46	1.58	2.11	1.49	1.61	2.16	1.51	1.63	2.16
q	2.17	2.45	3.76	2.31	2.62	4.12	2.45	2.80	4.50	2.49	2.86	4.64

Table 11 Values of the 5th, 10th and 50th percentiles of q^*, *OSR* and q–buildings with 1, 2 and 3 storeys, "flexural uncoupled" modelling

Percentile	$\theta_{u,shear}=0.20\%$			$\theta_{u,shear}=0.25\%$			$\theta_{u,shear}=0.30\%$			$\theta_{u,shear}=0.40\%$		
	5%	10%	50%	5%	10%	50%	5%	10%	50%	5%	10%	50%
N2 method												
q^*	1.16	1.37	2.48	1.28	1.53	2.86	1.44	1.70	3.38	1.75	2.11	4.09
OSR	1.14	1.22	1.55	1.14	1.22	1.55	1.17	1.25	1.59	1.16	1.24	1.57
q	1.62	1.96	3.80	1.79	2.18	4.37	2.12	2.60	5.32	2.51	3.08	6.37
Modified N2 method												
q^*	1.20	1.37	2.17	1.29	1.47	2.37	1.35	1.57	2.71	1.45	1.67	2.75
OSR	1.14	1.22	1.55	1.14	1.22	1.55	1.17	1.25	1.59	1.16	1.24	1.57
q	1.68	1.95	3.31	1.79	2.09	3.63	1.97	2.34	4.27	2.08	2.44	4.27

a function of the wall deformation limit failing in shear set in the analyses, equal to 0.20, 0.25, 0.30, and 0.40%. Table 12 resumes such values corresponding to the 10th percentile, showing the results as a function of the number of the storeys.

In general, the q-values are found to have a large range of variability, primarily depending on the structural configurations. In some cases, very large values of q can be found; these values are mainly due to the flexural behaviour of the walls. The parameter q^*, i.e., the basic value that takes into account the non-linear capacity of the structure, increases as the shear drift capacity increases, since shear failures govern the global seismic response of the considered buildings. On the other hand, the values of *OSR* do not vary significantly with the increase of the drift capacity. The N2 method in general provides values of q^* (and therefore of q) larger than the modified N2 method, above all for low-rise buildings and larger deformation capacities.

Moreover, it can be observed that, applying the N2 method, the values of q^* corresponding to one-storey buildings provide values about 20–30% larger than 2–3-storey buildings; with the use of the modified N2 method instead, the values of q^* do not increase significantly switching from one-storey to two/three storey buildings, since this method tends to reduce q^* for low rise/short period more than for high rise/large period structures. On the other hand, in the case of "flexural coupled" frame modelling, the values of *OSR* obtained

Table 12 Values of the 10th percentile of q^*, OSR and q

$\theta_{u,shear}$	"Flexural coupled" modelling								"Flexural uncoupled" modelling							
	N2 method			Modified N2 method					N2 method			Modified N2 method				
	q^*	OSR	q^*OSR	q	q^*	OSR	q^*OSR	q	q^*	OSR	q^*OSR	q	q^*	OSR	q^*OSR	q
1, 2 and 3 storey buildings																
0.20%	1.39	1.56	2.17	2.53	1.38	1.56	2.15	2.45	1.37	1.22	1.67	1.96	1.37	1.22	1.67	1.95
0.25%	1.53	1.58	2.42	2.85	1.45	1.58	2.29	2.62	1.53	1.22	1.87	2.18	1.47	1.22	1.79	2.09
0.30%	1.67	1.61	2.69	3.17	1.51	1.61	2.43	2.80	1.70	1.25	2.13	2.60	1.57	1.25	1.96	2.34
0.40%	1.96	1.63	3.19	3.71	1.54	1.63	2.51	2.86	2.11	1.24	2.62	3.08	1.67	1.24	2.07	2.44
1 storey—buildings																
0.20%	1.65	1.51	2.49	2.81	1.34	1.51	2.02	2.26	1.83	1.23	2.25	2.75	1.44	1.23	1.77	2.07
0.25%	1.86	1.54	2.86	3.21	1.39	1.54	2.14	2.39	2.12	1.24	2.63	3.18	1.51	1.24	1.87	2.18
0.30%	2.07	1.54	3.19	3.62	1.45	1.54	2.23	2.51	2.44	1.25	3.05	3.71	1.60	1.25	2.00	2.35
0.40%	2.41	1.58	3.81	4.32	1.46	1.58	2.31	2.58	2.95	1.25	3.69	4.44	1.63	1.25	2.04	2.37
2 storey—buildings																
0.20%	1.35	1.65	2.23	2.48	1.41	1.65	2.33	2.56	1.46	1.23	1.80	2.09	1.57	1.23	1.93	2.20
0.25%	1.48	1.67	2.47	2.77	1.49	1.67	2.49	2.76	1.58	1.24	1.96	2.18	1.62	1.24	2.01	2.22
0.30%	1.59	1.72	2.73	3.09	1.56	1.72	2.68	2.98	1.89	1.27	2.40	2.81	1.81	1.27	2.30	2.66
0.40%	1.89	1.72	3.25	3.61	1.58	1.72	2.72	3.00	2.26	1.27	2.87	3.31	1.85	1.27	2.35	2.68
3 storey—buildings																
0.20%	1.27	1.56	1.98	2.37	1.43	1.56	2.23	2.62	1.10	1.21	1.33	1.55	1.20	1.21	1.45	1.69
0.25%	1.39	1.58	2.20	2.63	1.54	1.58	2.43	2.87	1.25	1.21	1.51	1.79	1.36	1.21	1.65	1.94
0.30%	1.52	1.63	2.48	2.94	1.64	1.63	2.67	3.14	1.35	1.25	1.69	1.99	1.45	1.25	1.81	2.14
0.40%	1.75	1.63	2.85	3.37	1.69	1.63	2.75	3.22	1.50	1.25	1.88	2.47	1.7	1.25	2.13	2.45

for two–three storey buildings are about 10% higher than those for one-storey ones. Given these results, it seems reasonable to propose values of q-factors without differentiating with regard to the number of storeys. Regarding the two modelling approaches, it is possible to note that, as expected, the uncoupled models provide much lower values of *OSR* than the coupled ones (20–30% less), due to an inferior capacity of redistribution of the forces which is, at the 10th percentile, never larger than about 1.25. The values of q^* are instead in general slightly larger than the coupled models, especially on one and two-storey buildings, due to a higher probability of occurrence of flexural mechanisms. Figure 13 reports the values of the maximum attainable design PGA with the execution of pushover analyses for all the configurations computed according to Sect. 3.3, in relation to the most critical ground type. The figure shows the cases with deformation capacity for shear failures set equal to 0.20 and 0.40%.

In the case of "flexural coupled buildings", the values of the maximum attainable design PGA are found to be in the range between 0.087 and 0.331 g for two-storey buildings and between 0.074 and 0.206 g for three-storey configurations. Obviously, the reduction of the deformation limits for shear failures produces a decrease in the PGA "capacity" which, in some cases, is extremely large switching from 0.40% to 0.20%. For 0.20% of drift limit, the two-storey buildings provide average values of PGA capacity of about 0.16 g, with a minimum of 0.10 g in the case of building n.1, whereas the three-storey buildings produce average values of PGA capacity of about 0.12 g, with a minimum of 0.09 g in the case of building n.1.

In the case of "flexural uncoupled buildings", the values of the maximum design PGA are found to be in the range between 0.057 gand 0.182 g for two-storey buildings and between 0.054 and 0.150 g for three-storey configurations. For 0.20% of drift limit, no two-storey building attains values of PGA larger than 0.13 g and no three-storey building larger than 0.11 g, with minimum values of 0.06 and 0.05 g in the case of building n.1, respectively for the two-and three-storey configurations.

On average, the results of the N2 and the modified N2 method tend to be rather close in many situations, highlighting however an overall decrease of the PGA capacity of the modified N2 with respect to the N2 method in the case of two storey-buildings with 0.40% drift limit, and an increase of the PGA capacity in the case of three storey-buildings with 0.20% drift limit. This outcome is in line with the results of the inelastic displacement demand of SDOF systems discussed in Guerrini et al. (2017), that, as respect to the traditional N2 method, generally provides lower values of displacement demand for low values of ductility capacity of the system and flexible structures and larger values of displacement demands for larger values of ductility capacity and stiff structures.

6 Evaluation of the q-factor for "German" structural configurations

6.1 Structural configurations and material properties

The study for the evaluation of the q-factor for the "German" structural configurations is based on the preliminary work carried out within the research project ISEDEM (Butenweg

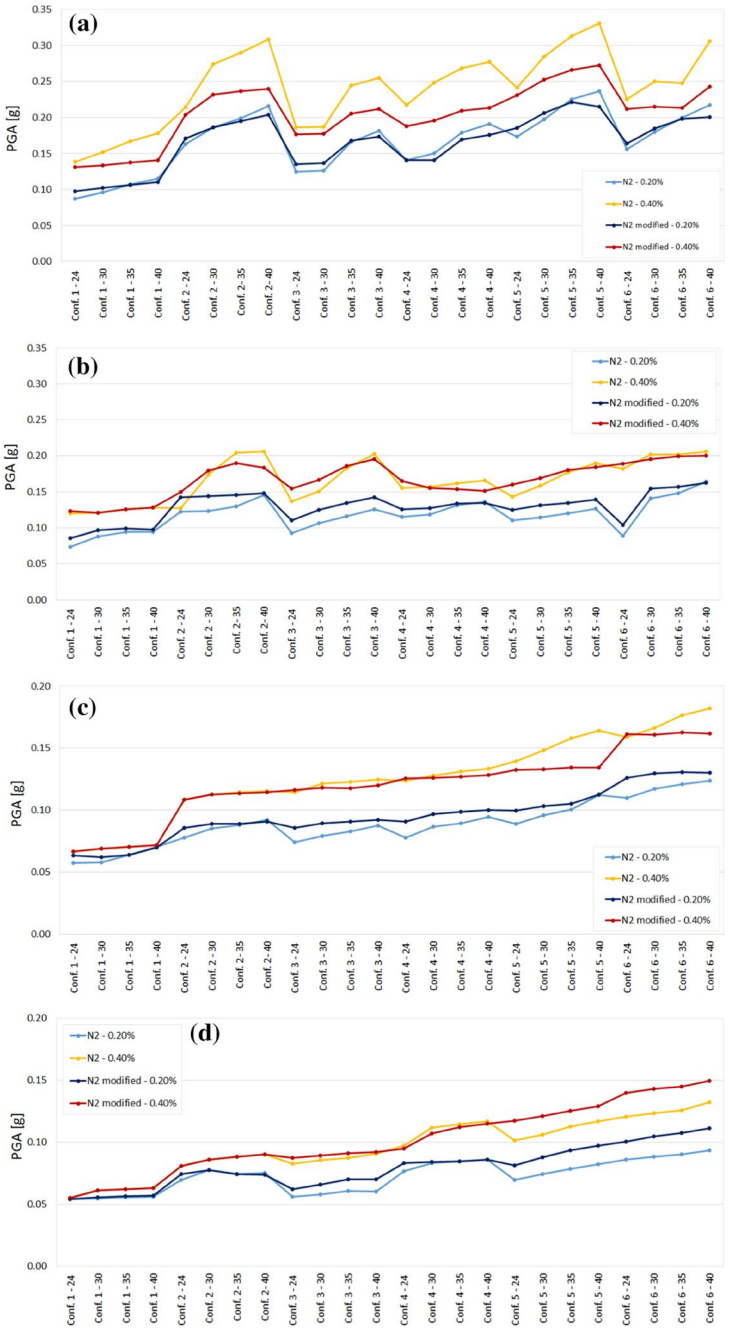

Fig. 13 Values of maximum attainable design PGA with pushover analyses for **a** "Coupled" buildings: two-storey buildings; **b** "Coupled" buildings: three-storey buildings; **c** "Uncoupled" buildings: two-storey buildings; **d** "Uncoupled" buildings: three-storey buildings

et al. 2019) which was financially supported by the German building authorities. A terraced, single-family and multi-family house with continuous shear walls and variable number of floors are considered for the brick types made of clay (CB), calcium silicate (CS), autoclaved aerated concrete (AAC) and lightweight concrete (LWC). The building configurations have been selected in close cooperation with the German masonry association DGfM. The building configurations can be regarded as representative for masonry buildings in Germany and provide a useful basis for the derivation of generally applicable behaviour factors. The resulting 28 building configurations are summarized in Table 13. The buildings are regular in elevation and can be also regarded as regular in plan. The total shear wall areas are ranging between 2.2 and 7.5% of the total floor area in each principal direction. The storey height in all buildings is 2.75 m and the continuous floors with a thickness of 180 mm are made of concrete with strength class C20/25 and reinforcement B500A. Figure 14 shows 3D views of the building typologies on the example of 09-FH-CS-1, 08-TH-CS-2 and 13-MFH-CS-3.

Table 14 provides the percentage of the shear wall areas relative to the floor area along X and Y ($\rho_{w,X}, \rho_{w,Y}$) and the seismic weight W of all configurations, calculated with the exclusion of the self-weight of half-height of the base walls. Table 15 summarizes the mean values of the strength parameters according to Eurocode 6 (CEN 2005b) in combination with the German National Annex DIN EN 1996–1-1/NA (DIN 2012) for all building configurations. The mean values have been calculated based on statistical data by using a conversion factor of 1.25 for the characteristic initial shear strength f_{vk0} and a factor of 1.20 for all other strength parameters. The masonry walls of all building configurations are constructed with un-mortared head-joints and thin bed mortar for the bed-joints.

The vertical loads and combination factors applied in the analyses of the building configurations are summarized in Table 16. Corresponding to the use as residential building, each storey is assumed to be independent and the factor φ is applied with 1.0 for the top floor and roof and with 0.7 for all other storeys according to DIN EN 1998–1/NA (2020). The combination factor ψ_2 is defined in accordance with EN 1990 (CEN 2002) except for snow loads. In contrast to EN 1990, the snow loads are combined with a combination factor of $\psi_2 = 0.5$. The mass of the roof for all investigated buildings is assumed to be smaller than 50% of the mass of the subjacent storey. Therefore, the roofs are simply considered as additional masses on the upper storeys instead of additional independent storeys.

6.2 Modelling approach and execution of pushover analyses

The overall building capacity is described by means of an inelastic static load-deformation curve under monotonously increasing horizontal loads. It is assumed that the failure mechanism takes part in the ground floor, characterized by a large inelastic drift while the upper stories remain linear elastic. Therefore, the overall capacity of the building is represented by the pushover curve of the ground floor, which is an appropriate assumption for buildings regular in plan and elevation. The pushover curve is calculated iteratively by imposing a displacement increment Δx in the direction of the seismic action. Afterwards, the resulting forces of all single shear walls are calculated using shear wall capacity curves. The typically non-symmetric wall configuration leads to torsional effects, which produces a rotation of the system around the centre of mass. In order to find the equilibrium, the system is rotated by $\Delta\varphi$ and translated by Δy in the perpendicular direction. The resulting pair of imposed displacement and reaction force in the direction of seismic action is a single point of the pushover curve. The overall

Table 13 Structural ground plan configurations of the parametric study. All dimensions in meters

	Terraced house (TH) 1-2 stories	Single-familily house (FH) 1-3 stories	Multi-family house (MFH) 2-4 stories
CB	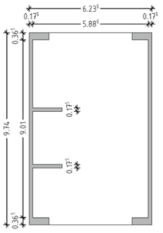	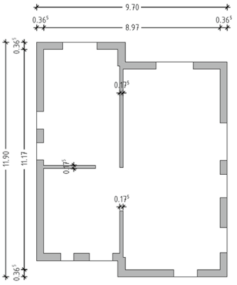	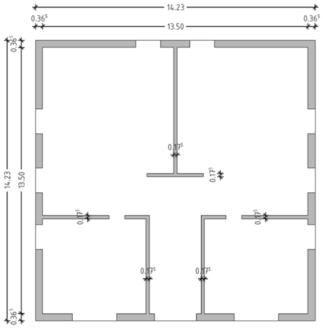
CS	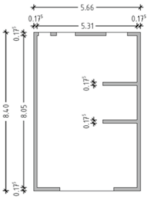	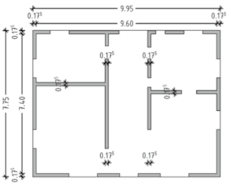	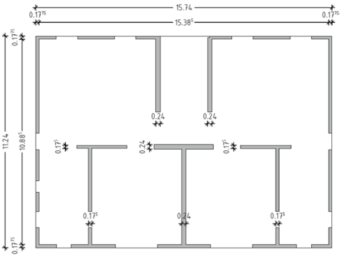
AAC	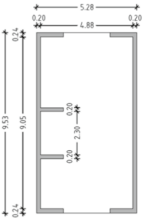	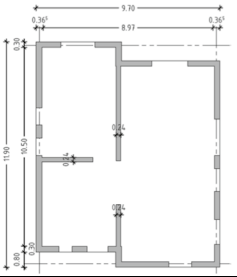	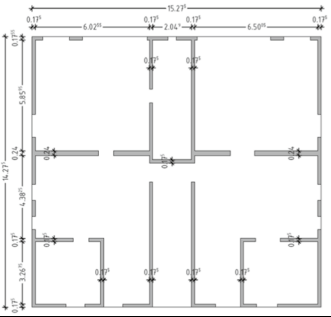
LWC	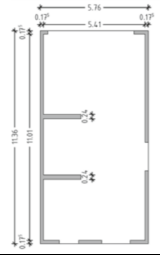	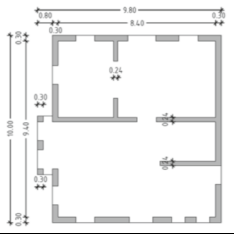	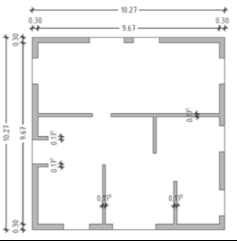

pushover curve is calculated by repeating the calculation for different displacements Δ_{GF} (Fig. 15). Similar to the building practice the contributions of spandrels and the interlocking effects of perpendicular walls are not considered. Therefore, wall sections with openings due to doors and windows are completely neglected. This is in line with the architectural trend of floor-high windows. Accidental torsional effects are simply

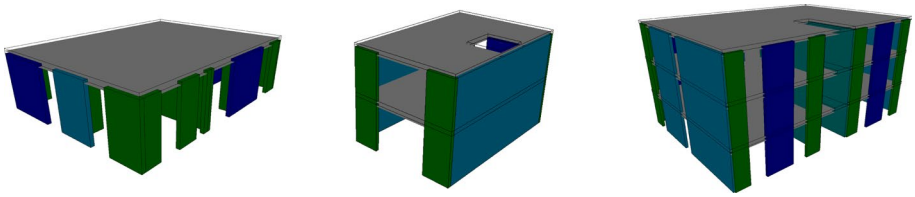

Fig. 14 3D views of the building configurations 09-FH-CS-1, 08-TH-CS-2, 13-MFH-CS-3

considered within the iteration scheme by imposing an eccentricity between the centre of mass and stiffness. Conservatively, the redistribution of vertical forces is not considered in the calculation.

The non-linear wall capacity curves are calculated according to DIN EN 1996–1-1/NA (2012) based on the resistances for bending and axial force (BA), shear due to friction failure (SS) and shear due to diagonal tension failure (ST). The bending resistance is calculated with the minimum reduction factor $\Phi_{OOP} = 0.9$ to account for out-of-plane eccentricities and slenderness of the walls according to Eurocode 6 (CEN 2005b). The deformation limits defined in terms of drift are determined with respect to the specific failure modes for shear and bending; two series of values have been considered, the second being in accordance with DIN EN 1998–1/NA (2020). The drift limits are defined with respect to the axial load ratio within the wall; the motivation for the choice of these drift values in case of shear response is reported in Sect. 7.1. The strength criteria and drift limits are summarized in Table 17.

The masonry wall is idealized as a Timoshenko beam element considering bending and shear deformations. The stiffness of the wall is defined by the superposition of the shear and bending stiffness of the equivalent beam. In the nonlinear range, cracked stiffness values for shear and bending are calculated with respect to the compressed length of the wall. For each applied displacement step the corresponding shear resistances are calculated as the minimum of the actual bending and shear resistances (V_{BA}, V_{SS}, V_{ST}). The moment distribution within the wall is described by the factor as the quotient of the shear span h_0 to the wall height h:

$$|M_u| \geq |M_o| : \psi = \frac{h_0}{h} = \frac{M_u}{M_u - M_o} \quad \text{and} \quad |M_o| > |M_u| : \psi = \frac{M_u}{M_o - M_u} \tag{20}$$

Figure 16 illustrates the overall deformation-controlled calculation using a tangent stiffness formulation. A detailed description of the calculation procedure is given in Butenweg et al. 2020. All the pushover analyses have been carried out using the software MINEA (SDA 2022).

6.3 Results of the analyses: *q*-factor and maximum attainable PGA

The 28 building configurations with 12 different ground plans, 1 to 4 storeys and brick types made of clay, calcium silicate, autoclaved aerated concrete and lightweight concrete have been analysed in the principle building directions with consideration of accidental eccentricities in two directions. The load pattern has been applied affine to the fundamental mode shape, which is continuously updated using the secant stiffness. Two response spectra with subsoil conditions C-R and C-S have been applied according to DIN EN 1998–1/NA (2020). The spectral shapes are defined by the expressions for the horizontal elastic response spectrum given in Eurocode 8 (CEN, 2005a) with control periods $T_C = 0.3$ s,

Table 14 Structural configurations, wall thicknesses, percentage of walls and total weight

Structural configurations	Thickness inner walls (mm)	Thickness outer walls (mm)	$p_{w,X}$(%)	$p_{w,Y}$(%)	W (kN)
01-TH-CB-2	175	365	3.5	5.2	1088
02-FH-CB-1	175	365	4.4	7.0	2139
03-FH-CB-2	175	365	4.4	7.0	2139
04-FH-CB-3	175	365	4.4	7.0	3132
05-MFH-CB-2	175	365	4.4	5.0	3799
06-MFH-CB-3	175	365	4.4	5.0	5539
07-MFH-CB-4	175	365	4.4	5.0	7279
08-TH-CS-2	175	175	3.3	5.9	966
09-FH-CS-1	175	175	3.9	4.6	1621
10-FH-CS-2	175	175	3.9	4.6	1621
11-FH-CS-3	175	175	3.9	4.6	2389
12-MFH-CS-2	175/240	175	2.7	4.4	3710
13-MFH-CS-3	175/240	175	2.7	4.4	5490
14-MFH-CS-4	175/240	175	2.7	4.4	7271
15-TH-AC-2	175	365	4.6	6.5	878
16-FH-AC-1	240	365	4.5	7.5	1936
17-FH-AC-2	240	365	4.5	7.5	1936
18-FH-AC-3	240	365	4.5	7.5	2794
19-MFH-AC-2	175/240	365	3.7	7.2	3875
20-MFH-AC-3	175/240	365	3.7	7.2	5598
21-MFH-AC-4	175/240	365	3.7	7.2	7321
22-TH-LWC-2	240	175	2.2	5.5	1314
23-FH-LWC-1	240	300	5.6	5.0	1855
24-FH-LWC-2	240	300	5.6	5.0	1855
25-FH-LWC-3	240	300	5.6	5.0	2717
26-MFH-LWC-2	175	300	5.3	4.7	2077
27-MFH-LWC-3	175	300	5.3	4.7	3035
28-MFH-LWC-4	175	300	5.3	4.7	3993

$T_D = 2.0$ s for C-R and $T_C = 0.5$ s, $T_D = 2.0$ s for C-S. The rising branch of the spectrum is neglected and the plateau range of both spectra has been applied between the $T = 0$ s and $T_C = 0.3$ s. A total number of 448 pushover analysis has been carried out to evaluate the basic values of q^* and OSR by using the CSM method. The values of the 5th, 10th, and 50th percentile have been calculated for OSR, q^* and q with and without flexural coupling elements subdivided according to the deformation limits failing in shear. As the deformation limits strongly depends on the vertical load level, the applied limits are defined with respect to the ratio of the vertical stresses σ_0 in the seismic design situation to the characteristic compressive strength of masonry f_k according to Table 17. Table 18 summarizes the mean values of axial load ratios σ_0/f_k [%] on the example of the building configurations for clay bricks with 2 to 4 storeys subdivided in inner and outer walls. The ratios are provided for the seismic design situation (S) and the persistent and variable design situation (P + V) as well. The axial load ratios of the outer walls in the seismic design situation vary between 2.5 and 5.95% in the ground floor, depending on the total number of

Table 15 Strength and stiffness parameters of different wall types used in the analyses

Configuration and wall thickness	f_b (MPa)	f_m (MPa)	$f_{bt,cal}$ (MPa)	f (MPa)	f_{v0} (MPa)	E (MPa)
TH-CB-1–2, t = 365 mm	12.80	10.00	0.33	5.28	0.275	4840
TH-CB-1–2, t = 175 mm	15	10.00	0.39	5.00	0.275	4950
FH-CB-1–3, t = 365 mm	12.80	10.00	0.33	5.28	0.275	4840
FH-CB-1–3, t = 175 mm	15	10.00	0.39	5.00	0.275	4950
MFH-CB-2–4, t = 365 mm	12.80	10.00	0.33	5.28	0.275	4840
MFH-CB-2–4, t = 175 mm	15	10.00	0.39	5.00	0.275	4950
TH-CS-1–2,t = 175 mm	15	10.00	0.30	7.00	0.310	5320
FH-CS-1–3, t = 175 mm	15	10.00	0.30	7.00	0.310	5320
MFH-CS-2–4, t = 240 mm	25	10.00	0.80	16.10	0.310	12,255
MFH-CS-2–4, t = 175 mm	25	10.00	0.80	16.10	0.310	12,255
TH-AC-1–2, t = 365 mm	2.50	10.00	0.08	1.80	0.220	792
TH-AC-1–2, t = 175 mm	5	10.00	0.16	3.00	0.220	1320
FH-AC-1–3, t = 365 mm	2.50	10.00	0.08	1.80	0.220	792
FH-AC-1–3, t = 240 mm	2.50	10.00	0.08	1.80	0.220	1320
MFH-AC-2–4, t = 365 mm	2.50	10.00	0.08	1.80	0.220	792
MFH-AC-2–4, t = 240/175 mm	5	10.00	0.16	3.00	0.220	1320
TH-LWC-1–2, t = 175 mm	25.0	10.00	0.80	12.50	0.314	9500
TH-LWC-1–2, t = 175 mm	2.50	10.00	0.08	1.875	0.314	1425
TH-LWC-1–2, t = 240 mm	2.50	10.00	0.80	12.50	0.314	9500
FH-LWC-1–3, t = 300 mm	2.50	10.00	0.08	1.875	0.314	1425
FH-LWC-1–3, t = 240 mm	25	10.00	0.80	12.50	0.314	9500
MFH-LWC-2–4, t = 300 mm	25	10.00	0.80	12.50	0.314	1425
MFH-LWC-2–4, t = 175 mm	5	10.00	0.10	1.875	0.314	9500

$f_{bt,cal}$: mean diagonal tensile strength of a masonry unit

storeys and the building typology. As expected, the inner walls show higher utilizations between 8.2 and 16.9%. Considering inner and outer walls together, the utilisations range from 6.4 to 9.77% in the seismic design situation. It has to be noted, that the ratios scatter for the inner walls, caused by the wall arrangement and the specific tributary areas of each wall. However, the utilisations in the seismic design situation for single walls do not exceed 10% for the outer and 21% for the inner walls the buildings under consideration. It can be concluded, that for the majority of shear walls the upper displacement limit for axial load ratios smaller than 15% applies.

Tables 19 and 20 summarize the results of the 5th, 10th, and 50th percentiles as the result for all considered configurations and Table 21 resumes the values corresponding to the 10th percentile as a function of the wall deformation limit failing in shear and the number of storeys. As a special building type, the results for the German terraced houses with few walls and quite different resistances in each building direction are provided, but not considered in the overall evaluation. The detailed evaluation of the results shows a large scatter of the basic value q^* that takes into account the deformation and dissipative capacity of the building. The value of q^* is mainly governed by the overall drift capacity of the building and the spectral shape. The overall drift capacity is usually limited by the shear drift capacity, except for buildings with flexural behaviour in case of shorter walls and lower vertical load levels. The main influencing parameter of the spectral shape is the control

Table 16 Gravity loads, variable loads and combination coefficients

	Floor load	Top floor	Roof structure
Slab system self-weight, g_{k1} (kN/m^2)	4.50	4.50	
Permanent actions, g_{k2} (kN/m^2)	1.50	1.50	1.70
Variable actions, q_k^* (kN/m^2)	2.70	2.70	0.45 (snow)**
φ–coefficient (–)	0.7	1.0	1.0
ψ_2–coefficient (–)	0.3	0.3	0.5

* Inclusive partition walls

** Roof pitch of 40°, snow load zone II, altitude of 245 m determined according to DIN EN 1991-1-3, NA (2010)

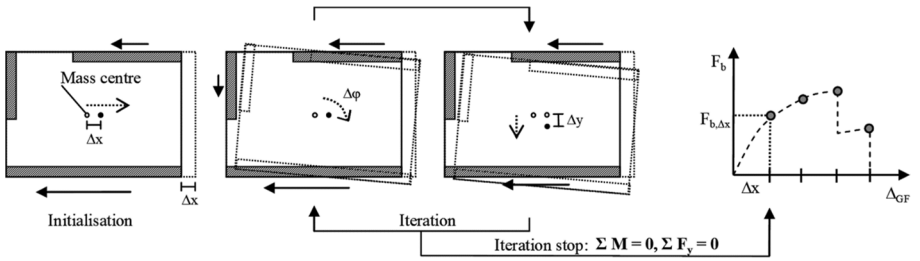

Fig. 15 Procedure for the calculation of the pushover curve for the ground floor (Mistler et al. 2007)

Table 17 Strength criteria according and ultimate displacements

	Resistance V_{Rd}	Ultimate deformation $\theta_u = d_u/h$
Bending and axial force (BA)	$V_{BA} = \frac{\sigma_0 l^2 t}{2\psi h}\left(1 - \frac{\sigma_0}{f_d \Phi_{OOP}}\right)$	$0.60\% \frac{h}{l}\psi$
Shear: Sliding (SS)	$V_S = f_{vd} l' \frac{1}{c}$ with $f_{vd} = \min(f_{vlt1}; f_{vlt2})$ Un-mortared head joints: $f_{vlt1} = 0,5 f_{v0} + 0,4 \cdot \sigma_{Dd}$	*CASE 1*: $\sigma_0 \le 0,15 f_k$: 0.25% $\sigma_0 > 0,15 f_k$: 0.20% *CASE 2:* $\sigma_0 \le 0,15 f_k$: 0.40% $\sigma_0 > 0,15 f_k$: 0.30%
Shear: Tension failure (ST)	$f_{vlt2} = 0,45 \cdot f_{bt,cal} \cdot \sqrt{1 + \frac{\sigma_{Dd}}{f_{bt,cal}}}$	

l, h, t: length, height and thickness of the wall; ψ: moment distribution factor ($=h_0/h$: shear span ratio); $f_d = f$: mean value of the compression strength of the masonry; σ_0 and σ_d: respectively, compression stress on the gross section ($\sigma_0 = N/(t \cdot l)$) and on the portion of the wall in compression ($\sigma_d = N/(t \cdot l')$, *N*: vertical load of the wall; Φ_{OOP}: reduction factor considering out-of-plane eccentricity and slenderness of the wall; f_{vd}: shear strength of masonry; f_{v0} mean value of the initial shear strength; l': compressed length of the wall calculated as $l' = \frac{3}{2}\left(1 - 2\frac{V_{Ed}}{N_{Ed}}\Psi\frac{h}{l}\right)l$; c: shear distribution factor; f_{vlt1}, f_{vlt2}: limit values of f_{vd}; $f_{bt,cal}$: tensile strength of a masonry unit; f_k: characteristic value of the compression strength of masonry

period T_c which increases for ground types with lower shear wave velocities. The increase of the control period T_c leads to a higher inelastic displacement demands that subsequently require a higher ductility of the building. In contrast, the values of *OSR* do not vary significantly with respect to the shear drift limit for one type of modelling for the investigated

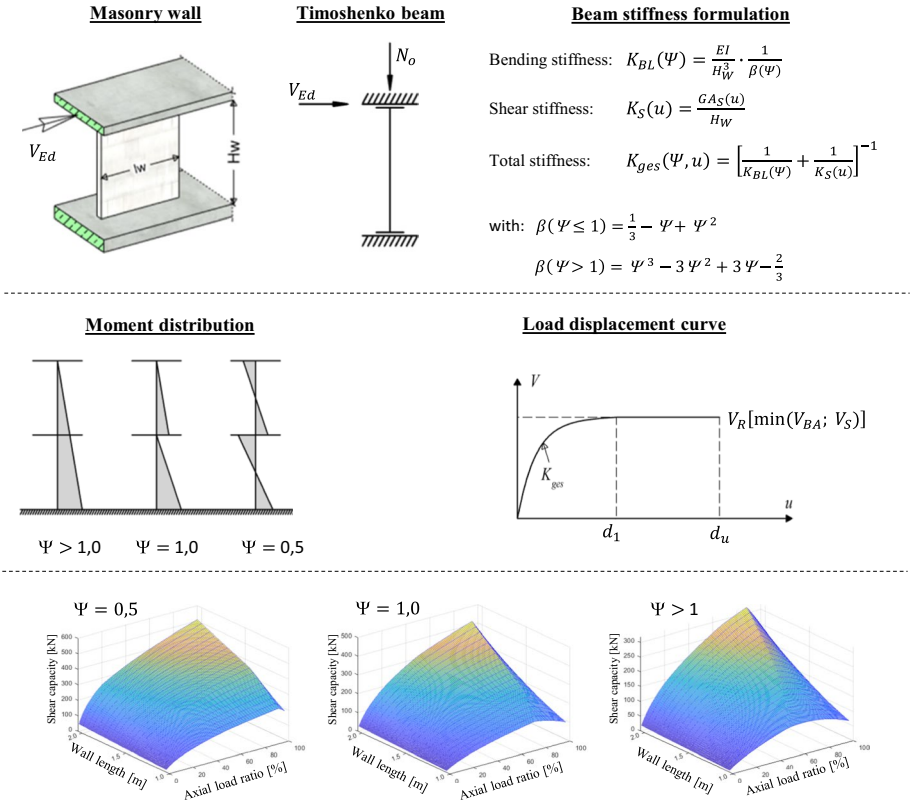

Fig. 16 Non-linear calculation procedure of wall capacity curves

Table 18 Mean values of utilisation σ_0/f_k [%] for inner, outer and all walls on ground floor level

Number of storeys		2		3		4	
Design situation		P+V	S	P+V	S	P+V	S
TH-CB	Outer	7.2	4.63	–		–	
	Inner	12.76	8.21	–		–	
	All	9.98	6.42	–		–	
FH-CB	Outer	3.86	2.50	5.69	–	-	
	Inner	16.06	10.39	23.66	15.21	–	
	All	6.37	4.12	9.38	6.03	–	
MFH-CB	Outer	4.82	3.11	7.08	4.53	9.34	5.95
	Inner	13.71	8.83	20.13	12.88	26.55	16.92
	All	7.91	5.10	11.62	7.43	15.33	9.77

one and multi-family houses. This results from comparable load redistribution potentials of these building types due to the variation of the wall lengths and axial load ratios. Rather low *OSR* values close to 1.0 have been obtained for the terraced houses with only two main shear walls in each building direction. In this specific case, the terraced houses may

Table 19 Values of the 5th, 10th and 50th percentiles of q^*, *OSR* and q–buildings with 1, 2, 3 and 4 storeys, "flexural coupled" modelling

Percentile	CSM—"Flexural coupled" modelling					
	$\theta_{u,shear}$			$\theta_{u,shear}$		
	$\sigma_0 \leq 0.15\ f_k$: 0.25% and $\sigma_0 > 0.15\ f_k$: 0.20%			$\sigma_0 \leq 0.15\ f_k$: 0.40% and $\sigma_0 > 0.15\ f_k$: 0.30%		
	5%	10%	50%	5%	10%	50%
q^*	1.38	1.42	1.67	1.63	1.69	2.09
OSR	1.48	1.50	1.66	1.50	1.51	1.66
q	2.33	2.39	3.08	2.67	2.78	3.63

collapse without further redistribution of horizontal forces due to the simultaneous failure of the main shear walls with identical lengths and comparable axial load ratios. This example clarifies that the calculated overstrength factors in the range of 1.5 can only be obtained with a sufficient number of walls with differing wall lengths and axial load ratios. However, it can be assumed that for most of the masonry buildings in practise, these criteria should be fulfilled. The overall comparison of the two modelling approaches shows larger OSR and q^* values for the buildings with flexural coupled elements.

Figure 17 shows the distributions of the maximum attainable design PGA for the building configurations with 2 to 4 storeys, flexural coupling and ground type C-R computed according to Sect. 3.3. The results are depicted in relation to the strong and weak building direction (SD/WD) and the upper displacement limits for shear failure of 0.25 and 0.40%. Obviously, the reduction of the displacement limits for shear failures produces a remarkable decrease of the maximum attainable design PGA. The amount of the decrease depends on the specific building configuration and cannot be described by a simple reduction factor. The main influencing parameter are the wall arrangement, wall lengths, axial load ratios, failure types of the walls and the spectral shape of the seismic input. The distribution of the building configurations without flexural coupling shows similar results (see Fig. 18), but in a lower level of maximum attainable design PGA, as the building behaviour is more flexural dominated with remarkable lower wall and overall building capacities.

7 Proposal for *q*-factor in seismic design codes

The values of q^*, *OSR* (α_u/α_1) and q have been estimated from the results of pushover analyses on different structural configurations, according to different deformation limits. Clearly, the evaluation of the q-factors cannot prescind by accurate estimation of the ultimate displacement capacity of the walls, which strongly affect the results of q^*. In particular, the in-plane drift capacity of the walls failing in shear controls the displacement capacity of the building in most of the cases, as reported in the results of the non-linear analyses, where q^* was found to increase as the drift capacity increases. Therefore, in order to propose a specific value of q, it is essential to provide proper values of drift limits for shear failure at ultimate conditions.

Table 20 Values of the 5th, 10th and 50th percentiles of q^*, *OSR* and q–buildings with 1, 2, 3 and 4 storeys, "flexural uncoupled" modelling

Percentile	CSM—"Flexural uncoupled" modelling					
	$\theta_{u,shear}$			$\theta_{u,shear}$		
	$\sigma_0 \le 0.15$ f_k: 0.25% and $\sigma_0 > 0.15$ f_k: 0.20%			$\sigma_0 \le 0.15$ f_k: 0.40% and $\sigma_0 > 0.15$ f_k: 0.30%		
	5%	10%	50%	5%	10%	50%
q^*	1.40	1.46	1.88	1.49	1.50	2.05
OSR	1.24	1.31	1.72	1.24	1.31	1.72
q	1.93	2.11	3.18	2.07	2.31	3.40

Table 21 Values of 10th percentile of q^*, *OSR* and q

$\theta_{u,shear}$	"Flexural coupled" modelling				"Flexural uncoupled" modelling			
	q^*	*OSR*	q^**OSR*	q	q^*	*OSR*	q^**OSR*	q
1, 2, 3, 4 storey buildings								
$\sigma_0 \le 0.15$ f_k: 0.25% $\sigma_0 > 0.15$ f_k: 0.20%	1.42	1.50	2.13	2.39	1.46	1.31	1.91	2.11
$\sigma_0 \le 0.15$ f_k: 0.40% $\sigma_0 > 0.15$ f_k: 0.30%	1.69	1.51	2.55	2.78	1.50	1.31	1.97	2.31
2 storey terraced buildings								
$\sigma_0 \le 0.15$ f_k: 0.25% $\sigma_0 > 0.15$ f_k: 0.20%	1.56	1.05	1.62	2.11	1.41	1.01	1.42	1.80
$\sigma_0 \le 0.15$ f_k: 0.40% $\sigma_0 > 0.15$ f_k: 0.30%	1.71	1.05	1.80	2.22	1.49	1.01	1.50	1.73
1 storey—buildings								
$\sigma_0 \le 0.15$ f_k: 0.25% $\sigma_0 > 0.15$ f_k: 0.20%	1.50	1.50	2.25	2.37	1.45	1.20	1.74	1.78
$\sigma_0 \le 0.15$ f_k: 0.40% $\sigma_0 > 0.15$ f_k: 0.30%	1.63	1.50	2.45	2.46	1.48	1.20	1.78	1.84
2 storey—buildings								
$\sigma_0 \le 0.15$ f_k: 0.25% $\sigma_0 > 0.15$ f_k: 0.20%	1.50	1.46	2.19	2.34	1.47	1.25	1.84	1.93
$\sigma_0 \le 0.15$ f_k: 0.40% $\sigma_0 > 0.15$ f_k: 0.30%	1.76	1.52	2.68	2.81	1.54	1.25	1.93	2.35
3 storey—buildings								
$\sigma_0 \le 0.15$ f_k: 0.25% $\sigma_0 > 0.15$ f_k: 0.20%	1.41	1.50	2.17	2.45	1.40	1.38	1.93	2.45
$\sigma_0 \le 0.15$ f_k: 0.40% $\sigma_0 > 0.15$ f_k: 0.30%	1.79	1.50	2.69	2.97	1.50	1.38	2.07	2.69
4 storey—buildings								
$\sigma_0 \le 0.15$ f_k: 0.25% $\sigma_0 > 0.15$ f_k: 0.20%	1.39	1.52	2.11	2.41	1.47	1.31	1.93	2.83
$\sigma_0 \le 0{,}15$ f_k: 040% $\sigma_0 > 0.15$ f_k: 0.30%	1.71	1.52	2.60	3.02	1.61	1.31	2.11	2.95

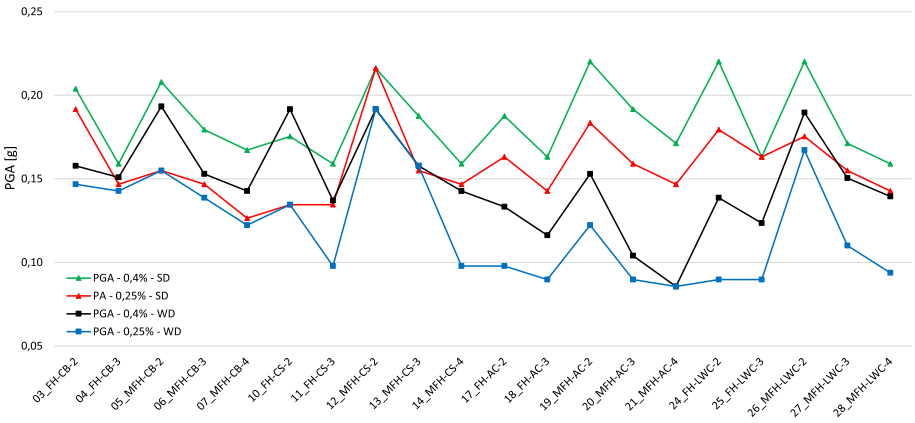

Fig. 17 Maximum attainable design PGA for coupled flexural modelling for all building configurations in strong and weak building direction (SD/WD) for ground type CR

7.1 Evaluation of *q**: considerations on drift limits for shear mechanisms

The drift capacity is usually estimated through a suitable interpretation of in-plane cyclic tests on walls. In this regard, a research characterized by the development of a dataset collecting the results of in-plane cyclic tests on 188 URM piers with different masonry typologies has been recently carried out by Morandi et al. (2018), where specimens built with vertical Hollow Clay (HC), Autoclaved Aerated Concrete (AAC), Calcium-Silicate (CS), Lightweight Aerated Concrete (LAC) blocks and Clay Solid Brick (SB-C) have been considered. On the envelopes of the experimental response on each pier, different points have been selected as representative of different limit states. In this study, the interest lies on the Severe Damage limit state (SD) since, according to the recent codes (NTC2018; draft EC8 1–2, CEN 2019b), the safety verifications on masonry elements with the application of linear analyses with q-factor need to be performed at SD, under the assumption/condition that, once SD is fulfilled, also the Near Collapse limits state (NC) is implicitly satisfied.

In earlier experimental research works on the subject, the ultimate drift capacity of walls was associated to the value of deformation corresponding to strength degradation of 20% after the peaki ($\alpha_{20\%drop}$), but no thorough discussion was made on whether this limit has to be considered associated to a SD or a NC limit state. The definition of proper limits at SD and NC on the post-peak experimental envelope is still controversial, since the in-plane response of the walls is strongly affected by several parameters and may be characterized, for weak failure modes, either by post-peak branches with gradual force degradation or by sudden decays after the peak. For example, vertically hollowed clay masonry piers tested by Morandi et al. 2019 (typology "MA"), failed by shear, provided strength reduction up to more than 50%, with drift values significantly larger than those at 20% of degradation (from about 2 to 4 times larger), still guaranteeing some reserve capacity against vertical loads; on the other hand, some other types of masonry showed a sudden decay after the peak force with limited increment of deformation capacity after 20% of drop (see, e.g., Petry and Beyer, 2014). Although wider investigation on this topic is surely still needed, the Severe Damage limit state is here associated to the value of deformation corresponding to a strength degradation of 20% after the peak, considering also that in the vast majority of

experimental tests, the development of visible shear cracking corresponds just about to the attainment of the peak shear force capacity.

Different experimental failure modes have been found in the tests (flexural, shear, and hybrid shear/flexural mechanisms), but since shear failures govern the global seismic response of the considered buildings, an estimation of the limits for shear at SD is essential. From the analysis of the aforementioned test campaigns, but also from other experimental experiences (see, e.g., Fasching et al. 2020), it is evident that the drift limits for shear failures at SD lie in a wide range depending on several parameters, such as the typologies and characteristics of the masonry and of the head-joints (filled, dry, with tongue and groove), the vertical axial load ratio, the shear span to wall height ratio which, in its turn, depends on the moment distribution on the wall. Although a unanimous consensus on the evaluation of such deformation limits is not achieved yet and further studies are ongoing, the results of the tests clearly show that the drift limits for shear failures at SD can be reasonably set ranging between 0.20 and 0.40%.

7.2 Proposal for *q* factor

Given the range of values of displacement capacity of the walls failing in shear discussed in the previous section and according to the results of the pushover analyses conducted on the Italian (Tables 10, 11 and 12) and German configurations (Tables 19, 20 and 21), design values of q^*, OSR (α_u/α_1) and q are here proposed. It seems reasonable with respect to the engineering practise to propose the values of q-factors without differentiating on the number of storeys. For the Italian and German configurations, the proposed values of q-factors are reported respectively in Tables 22 and 23. They have been estimated as a low precautionary percentile of the results, in particular, equal to the 10th-fractile on "flexural coupled" models, since provide results for q^* slightly lower than the "uncouple" models. For the Italian configurations the minimum between the results provided by the N2 and the modified N2 method has been considered (Table 9). In the case of building configurations

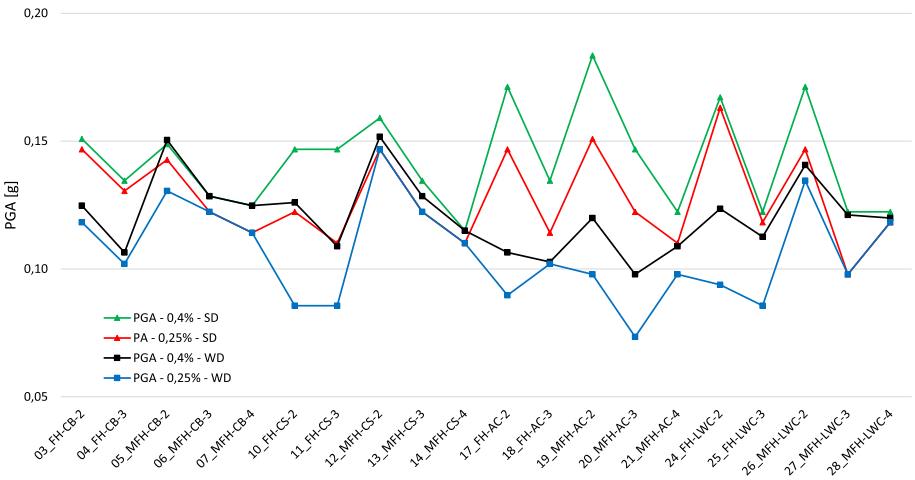

Fig. 18 Maximum attainable design PGA for uncoupled flexural modelling for all building configurations in strong and weak building direction (SD/WD) for ground type CR

Table 22 Proposed values for q-factor (Italian Configurations)

$\theta_{SD,shear}$ (%)	q^* (–)	OSR (α_u/α_1) (–)	$q^*{\cdot}OSR$ (–)	q (–)
0.20	1.35	1.60	2.16	2.45
0.25	1.40	1.60	2.24	2.60
0.30	1.50	1.60	2.40	2.80
0.35	*1.55*	*1.60*	*2.48*	*2.85*
0.40	1.60	1.60	2.56	2.90

Italics: Interpolated values

that can exploit a full redistribution of the forces, as for the buildings considered in the evaluations, the values of q-factors can be taken as the values at the rightmost column of Table 22 and Table 23. It can be noticed that the product $q^*{\cdot}OSR$ considering separately the 10th-fractile values of q^* and OSR is lower than the 10th-fractile value of the overall q-factor, since this latter is derived for situations where the minimum contributions of q^* and OSR do not occur simultaneously. On the other hand, in the case of configurations where the redistribution of the forces is not possible or it is limited, it is only feasible to use the value of q^*, eventually multiplied by a reduced value of OSR. This aspect was already discussed in Sect. 6.3 on the example of the terraced houses in Germany. The comparison of the Italian and German studies for the design values of q^*, OSR (α_u/α_1) and q on different building configurations, brick types and spectral shapes, different simulation models and different approaches to estimate the inelastic displacement demand (N2, modified N2, CSM) shows a good agreement. Overall, the results of the German study provide slightly more conservative results with 5–10% lower design values of q^*, OSR and q. The good agreement results from the application of the same approach to derive the three behaviour components and the fact that both calculation models are able to represent the shear and bending failure modes of the walls, the frame actions due to the interaction with the slabs and the load redistribution in the nonlinear range. Furthermore, it must be taken into account that identical ultimate displacement capacities in shear are applied, which are the main influencing parameter on the results. Finally, it should be noted that despite similar behaviour factors, the two approaches may result to different maximum attainable design PGAs because the calculation of the wall resistances differs.

The calculated values are applicable only for buildings regular in elevation and almost regular in plan. The values of q-factor should be properly reduced if the building is irregular. If the building is irregular in elevation, a reduction coefficient of 0.80 can be applied, if it is also irregular in plan, a further reduction of 0.80 can be considered suitable. Furthermore, the proposed tables are only applicable for buildings with a sufficient number of walls with differing wall lengths and axial load ratios. Finally, it should be pointed out once again, that the given design values of q^*, OSR and q are lower bound values as a result of the required generalization in the design codes.

7.3 Definition of the *q*-factor according to Eurocode 8

According to the draft of EC8-Part 1 (CEN 2019a), the q-factor can be written as a product of three factors:

$$q = q_D \cdot q_R \cdot q_S \tag{21}$$

Table 23 Proposed values for q-factor (German Configurations)

$\theta_{SD,shear}$ (%)	q^* (–)	OSR (α_u/α_1) (–)	$q^*{\cdot}OSR$ (–)	q (–)
0.25	1.40	1.50	2.10	2.40
0.30	*1.50*	*1.50*	*2.25*	*2.55*
0.35	*1.60*	*1.50*	*2.40*	*2.65*
0.40	1.70	1.50	2.55	2.80

Italics: Interpolated values

where q_D is the behaviour factor component for the deformation and energy dissipation capacity ($=q^*$), q_R is the behaviour factor component accounting for overstrength due to the redistribution of seismic action effects in redundant structures ($=OSR=\alpha_u/\alpha_1$) and q_S is the behaviour factor component accounting for overstrength due to all other sources. While on the contributions of $q_D=q^*$ and $q_R=OSR$ a wide discussion is already done, some considerations on q_S are reported in the following section. Figure 19 shows the three behaviour factor components similar to the former definition.

7.3.1 Considerations on q_s factor

The factor q_S accounts to a large extent for the material overstrength, as well as for excess resistance due to unavoidable overdesign of sections (i.e., always the next larger section is chosen). For URM buildings, it is assumed that the q_S factor can be affected by the contribution of the material safety factors in the safety checks and by all those effects that increase the strength but are typically not accounted for when modelling masonry buildings. Furthermore, the accuracy of the analytical approaches for the estimation of the shear resistance in the design can affect the overstrength.

The strength of URM elements failing in flexure is almost exclusively affected by the axial force with a very low contribution of the compression strength of the masonry, at least for the low to moderate axial load ratios. For this reason, if all walls in a building would fail in flexure, the component of q_S resulting from overstrength due to the use of the material safety factor should be about equal to unity. On the other hand, for URM walls failing in shear, the lateral resistance depends on both the axial force and the assumed material properties. The shear strength obtained with characteristic values divided by partial safety factors is, on average, $1.25\gamma_m$ -times lower than the mean actual shear strength (expected value), being 1.25 the ratio between mean and characteristic strength value (as also proposed in material testing standards). The partial safety factors can vary in each country, however, the minimum permitted partial safety factor for masonry in the current EC8 is $\gamma_m=1.5$ and a minimum value of 2.0 is used in most countries; this can lead to a total ratio between mean and design value of 1.875–2.50. In the special case of Germany, the partial safety factor in the seismic design situation is defined only with $\gamma_m=1.2$ which leads to a reduction of the total ratio to 1.44. The reduction of material strength parameters does not provide a proportional reduction of the strength of a wall (shear failures and flexural failures have different sensitivity to material strength parameters, where flexural failure is less sensitive than shear failure). Similarly, the system strength can vary in function of the predominant failure mechanism. Considering that the drift ratios that dictate the values of q^* are those associated to shear failures and assuming that in a building the system capacity is affected mostly by shear failures, typically associated to the longer and stronger

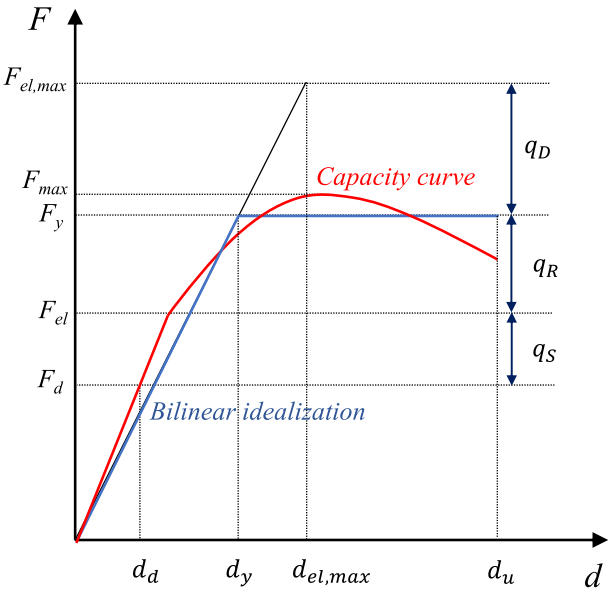

Fig. 19 Definition of the behaviour factor components q_D, q_R and q_S

walls, a safe estimate of the effect of material strength reduction from mean to design value would affect the system capacity by a factor up to 1.1–1.2. An example of the contribution of different safety factors on the strength properties has been carried out on the configuration n. 5 of Fig. 9 (two-storey building, wall thickness = 300 mm), considering the mean values and the design values (characteristic values divided by $\gamma_m = 1.5$, 2.0, and 2.5) of the masonry strength reported in Table 7. The capacity curves and the results of the ratios $F_{el,mean}/F_{el}$ of Fig. 20 refer to pushover analyses conducted in + X direction, with a positive accidental eccentricity and an inverse modal triangular lateral distribution of forces.

Another potential cause of overstrength was identified by the comparison of lateral resistances determined with shear wall tests and calculated according to EC6 (2005b). Morandi et al. 2018 showed that the experimental strength calculated by EC6 equations for walls failing in shear is pretty well-predicted when using mean material parameters; the analytically predicted lateral strength was equal to or lower than the lateral resistances of the experimental shear wall tests for about 60% of the specimen. Similar results were obtained by a detailed evaluation of 48 shear wall tests on masonry walls made of typical hollow clay bricks available on the German market (Lutman 2018, 2019, 2020; Fehling and Stürz 2007). However, the conservatism of the normative resistances and their influence on the overstrength depends on the national regulations and specific country products and cannot be easily generalized here.

Some other effects can increase the horizontal load bearing capacity of a masonry building, but are typically not explicitly modelled and can be therefore also attributed to the q_S component. Such effects are for example the coupling effect of ring beams and of spandrels (ring beams are sometimes modelled as an axial member and not as a flexural member, masonry spandrels are often neglected), the coupling provided by the flexural stiffness of floors, which is usually neglected, the flange effects, i.e., the composite action of orthogonal walls intersecting at vertical edges, and kinematic effects associated to uplifting (rocking) of walls failing in flexure with limited axial force. The magnitude of these effects may vary significantly between buildings and models, but it can be reasonably assumed in the

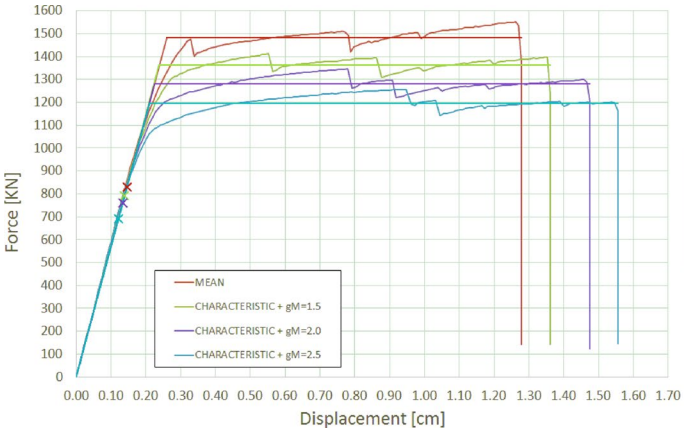

Material properties	F_{el} [kN]	$F_{el,Mean}/F_{el}$ [kN]
Mean	830	1.00
Characterstic + γ_M=1.5	792	1.05
Characterstic + γ_M=2.0	760	1.09
Characterstic + γ_M=2.5	690	1.20

Fig. 20 Capacity curves with different values of strength properties and ratios $F_{el,mean}/F_{el}$

order of at least 1.1–1.2, the lower values apply when coupling of ring-beams or floors is explicitly modelled, the larger when they are neglected.

Considering also the effect of material strength reduction from mean to design value, the underestimation of resistances using simplified analytical design approaches in design codes and simplified modelling approaches, a total q_S of about 1.3–1.5 can be justified in conjunction with a q^* dictated by shear failures, depending on whether the flexural coupling given by ring beams or floors is explicitly considered or not. Such a parameter can be therefore taken into account to further increase the q-factor.

Given all that, the authors believe that a minimum value of overstrength $q_R \cdot q_S$ equal to 1.50 can be always employed, also in case of structural configurations unable or with limited capacity to exploit the overstrength provided by the redistribution of the forces.

7.4 Justification of *q*-factor values: experimental and earthquake experience and evaluation of the annual probability of near collapse of URM buildings

7.4.1 Experimental evaluation of *q*-factor

In the European context, important experimental references for the evaluation of behaviour factors for *URM* masonry buildings can be found in early researches carried out in Slovenia by Tomaževic et al. (Tomaževič and Weiss 1994; Tomaževič 1999; Tomaževič et al. 2004) and in Italy by Benedetti et al. (Benedetti and Castoldi 1982; Benedetti et al. 1998).

From such experimental tests carried out on scaled specimens of buildings subjected to dynamic actions through shaking-table tests, it was evident that the values of behaviour factor q^* for URM buildings well-constructed and that guarantee their "box" behaviour are in the range between 2.0 and 2.5; a strong irregularity can produce a decrease of the behaviour factor of about 30%.

Moreover, a re-exam of the dynamic tests carried out by Benedetti (2004) in the '80s and '90s, led to a conclusion that the values of the overstrength ratios OSR ($=F_y/F_{el}$) are in line with what obtained numerically. From this re-exam, the author stated that the overstrength ratio can be prudentially evaluated about the value of 1.3 (Benedetti 2004), although, from

the observations of the experimental tests by Benedetti, it can be noticed that values of about 1.6 were also attained for regular buildings with suitable structural and construction details. It is however important to underline that the definition of the base shear corresponding to the first wall of the building that attains its flexural or shear strength (F_{el}) in an experimental test is subjected to large uncertainty. It is often very difficult to evaluate the first occurrence of a failure in the masonry structural elements during an experimental test on models (opening of the first crack ?, crushing of the masonry ?, sliding ?). Nevertheless, as already mentioned, the quantitative evaluation of the overstrength to be used for the calculations cannot leave out considerations coming from numerical analyses, because it is strongly related to the model assumptions and the strength criteria.

In conclusion, based on these test results, it is possible to state that the level of the reduction of the elastic forces for *URM* buildings well organized and that provide a "box" behaviour is at least 2.5–3.0 obtained as the product of a basic q_0 of 1.5–2.0 multiplied by an overstrength ratio *OSR* of about 1.5.

7.4.2 Earthquake experience

As discussed in more detail in the introduction, the response of modern masonry buildings in recent earthquakes was found to be satisfactory, in some cases up to rather large levels of seismic action.

A recent study has analysed in detail the seismic performance of three modern URM buildings struck by the earthquake sequence in Emilia, as reported in Rosin et al. (2018) and Morandi et al. (2020). Linear and non-linear analyses were conducted on such buildings. The results for the two buildings regular in elevation are reported in Table 24. In the case of linear analyses according to the Italian (NTC 2008), a q-factor of 2.8 was set for the building "Pr3" (with irregularity in plan) and 3.6 for the building "Po1" (regular in plan and elevation). With the application of linear analyses on an equivalent frame modelling of the structure and without redistribution of the forces, very small values of maximum attainable design PGAs were obtained (in all cases less than 0.05 g), found to be significantly lower than the effective seismic action that struck the buildings, which did not cause any visible damage or cracking in the masonry elements of the two buildings regular in elevation. More information can be found in Morandi et al. (2020).

7.4.3 Results of annual probability of collapse from probabilistic seismic assessment

In order to check the validity of the elastic analyses with different values of q-factor, it is of interest to look at works in the literature where probabilistic seismic assessment that derives the annual probability of collapse of newly designed URM buildings was carried out.

In recent years an extensive coordinated project to evaluate the seismic risk of code-conforming buildings was carried out in Italy (Iervolino et al. 2018; Franchin et al. 2018; Manzini et al. 2018; Cattari et al. 2018) with reference to the Italian norms NTC2008. In such a study, the annual probability of collapse p_{NC} (or rate of collapse) of URM masonry buildings designed following different methods of analysis (namely linear elastic with q-factor or nonlinear static) was calculated. The buildings were "just designed" for the different seismic hazard levels and site conditions. As stated above, NTC2008 assumed values of q for regular URM buildings equal to 3.6 for two- and three-storey, as a result of

Table 24 Maximum attained PGA and seismic demand for each building (Morandi et al. 2020)

Building	Max attained PGA [g]		Design PGA_{475} [g]	Estimated PGA [g] from May 2012 earthquakes			
	Linear elastic—Eq. Frame -	Non-linear static—Eq. Frame -		20.05.2012—EW	20.05.2012—NS	29.05.2012—EW	29.05.2012—NS
Pr3	0.032	0.173	0.277	0.211	0.214	0.171	0.170
Po1	0.048	0.243	0.218	0.349	0.338	0.275	0.284

Table 25 Annual probability of collapse p_{NC} for URM buildings designed with linear analysis as per NTC 2008 (Iervolino et al. 2018; Manzini et al. 2018; Cattari et al. 2018)

	Site		
	Caltanissetta, Italy	Rome, Italy	Naples, Italy
Soil type	A	A	A
$S_a(T_1)_{475}$ (PGA_{475})	0.19 g (0.073 g)	0.28 g (0.110 g)	0.40 g (0.168 g)
Building 2 (3 storeys)	1.79×10^{-5}	–	–
Building 8 (2 storeys)	–	–	3.64×10^{-5}*
Building 8 (3 storeys)	1.13×10^{-5}	1.45×10^{-5}	–
Building 9 (2 storeys)	–	1.01×10^{-5}	–
Building 9 (3 storeys)	2.97×10^{-5}	–	–

*Capacity/demand ratio in linear design = 0.96

a $q^*=2.0$ and $\alpha_u/\alpha_1=1.8$, resulting from an estimate of ultimate deformation capacity of URM walls which were essentially based on older experiments on solid brick URM walls. In fact, in the probabilistic study, the median drift capacity at Near Collapse of URM walls was assumed equal to 0.54%, and the assumed standard deviation was producing (lognormal distribution) a 5% percentile that would result in 0.35% drift. The cases of URM buildings designed with linear analysis and q-factor with no force redistribution provided p_{NC} values ranging from about 1.0×10^{-5} to 3.6×10^{-5}, as reported in Table 25.

Studies where lower drift capacities are used for the probabilistic assessment, in line with the more recent experimental results on modern masonry (e.g., hollow units), are still underway. A preliminary investigation of the collapse rate p_{NC} with a probabilistic procedure on real modern URM buildings with hollowed clay units re-designed according to NTC2008, has been carried out with reference to the two buildings considered in Sect. 7.4.2 hit by the 2012 seismic events in Emilia (see Butenweg et. al. 2018; Kallioras et al. 2018a). In this probabilistic assessment, static and dynamic non-linear analyses were conducted, assuming a median drift capacity at the ultimate condition of URM walls equal to 0.29% for building "Pr3" and 0.38% for building "Po1". Both buildings provided very low values of the maximum attained design PGA when analysed with linear analyses on equivalent frame modelling using a q-factor equal to 2.8 for Pr3 and to 3.6 for Po1. The buildings were then assumed to be "detached" from their effective construction sites (in Emilia) and different locations with a seismic hazard that provided values of PGA at $T_R=475$ years equal to maximum attained design PGA from linear analyses were searched and found in Germany with the aid of "SHARE" (Giardini et al. 2014). The values of the annual probability of collapse, for the cases of URM buildings designed with linear analysis and q-factor with no force redistribution, were found to be about 0.1×10^{-5} and 0.34×10^{-5} (see Table 26). Such values are very small due to the low performance of those buildings from linear analyses, in their turn characterized by very low hazard sites.

If, for instance, the target annual probability of collapse is taken equal to 2×10^{-4} as recommended in prEN1998-1–1 (CEN 2019a) for ordinary buildings designed according to Eurocode 8, the actual probability of collapse p_{NC} obtained in the previous studies is at least one order of magnitude smaller. This leads again to support the use of total q-factors greater than 2.0 for the linear elastic design of URM buildings.

Table 26 Annual probability of collapse p_{NC} for URM buildings designed with linear analysis as per NTC2008 (Kallioras et al. 2018b)

	Site	
	Mücheln, Germany	Hof, Bayern, Germany
Soil type	A	A
$S_a(T_1)_{475}$ (PGA_{475})	0.08 g (0.032 g)	0.12 g (0.048 g)
Pr3 (*q-factor* = 2.8)	0.34×10^{-5}	–
Po1 (*q-factor* = 3.6)	–	0.11×10^{-5}

7.5 The role of the force redistribution after linear analyses

The recognition of the necessity of the "overstrength ratio" $OSR = \alpha_u/\alpha_1$ in masonry design/assessment, formerly introduced in the Italian norms in 2005 (OPCM 2003), was certainly an important step to rationally explain and find a rapid solution for the inconsistencies found in the application of the code. Nevertheless, the choice of a specific value of α_u/α_1, even for the same homogeneous typology of masonry buildings, does not overcome completely the intrinsic problems of the linear methods of analysis. Considering a homogeneous class of masonry buildings, the choice of a single conservative value, be it a "sufficiently conservative" percentile (e.g., 10th percentile), has the consequence that in the wide majority of the cases, in which the α_u/α_1 is much higher (e.g., 2.0 or 3.0), the design seismic action would be much higher than it should. For such configurations, the use of a default conservative α_u/α_1 could be so penalizing that the strength safety checks can never be satisfied, even if the quality of materials, the structural configuration and details, the total amount of shear walls clearly show that the design should be safe.

In such a situation, it is very useful to resort to a redistribution of internal forces after the linear elastic analysis is carried out. This possibility was considered by design codes, including EC8, since the very early drafts. However, the limits to force redistribution in EC8 have been so far so strict to make redistribution almost ineffective in many practical problems; in particular, the limit of 25% in the maximum reduction of the shear in any wall is useless in many practical situations, for example when one wall carrying a limited percentage of the total inter-storey shear does not satisfy the strength check because the vertical load on it is low, and strength is mainly determined by geometry and vertical load. The origin of these limits dates back to 1985 or earlier, at times in which the experience in the nonlinear analysis was quite limited, and recalls criteria originally developed for reinforced concrete structures.

The problem of elastic analysis is that it does not provide a correct distribution of internal forces with reference to ultimate limit state, and that differences with more accurate nonlinear analyses tend to be much higher than the limits imposed for redistribution. It must be remarked that more rational solutions could be envisaged, such as those being explored in Morandi 2006, where the possibility of overcoming the use of the α_u/α_1 is attempted, allowing a larger redistribution which could allocate shears approaching the available strength reserve of the walls, as would be the result of nonlinear analysis. Nevertheless, a balance between α_u/α_1 ratio and the limit to force redistribution should be sought, in order not to produce unconservative designs.

In the Italian Norms of the last 15 years, the revised OPCM 3431 in 2005, the more recent NTC2008 and the current NTC2018, the limits to force redistribution have been relaxed, stating that the variation in shear in each wall should not exceed the largest

value between 25% of the shear in the wall and 10% of the total inter-storey shear. In the case of non-rigid diaphragms, the redistribution is allowed only among coplanar walls connected by ties or r.c. beams (in such case the inter-storey shear is evaluated considering only the contribution of the coplanar walls). Such choice, motivated by the need to find an urgent remedy to the inconsistent over-conservative results that can be obtained by using linear analysis, was based on the comparison of linear and nonlinear analyses.

One way to encompass the wide range of possible floor plan layouts could be to set α_u/α_1 ratio equal to 1.0, allowing at the same time a wide redistribution of the forces between the walls which would approach the distribution that would be obtained from a nonlinear analysis. This would clearly be possible only if there is redundancy and if the redistribution does not implicitly violate the deformability limits of walls. Provided a method is developed to account for limited deformation capacity when setting limits on the redistribution of the forces, this would be an appealing alternative to using the heuristically based α_u/α_1 factors derived from the analyses on sets of buildings with specific configurations. Work on this approach is under development at the University of Pavia.

In order to summarize all the possible cases, the three following solutions are viable in masonry buildings where redistribution is possible:

- if α_u/α_1 is evaluated from a pushover analysis, no further redistribution is possible;
- if α_u/α_1 is set equal to the conservative estimation derived from the analyses of the considered configurations, as done in this article, a limited redistribution is possible;
- if α_u/α_1 is set equal to 1.0, a wider redistribution of the forces is allowed.

8 Conclusions

The verification of low-rise URM buildings with linear elastic analysis and behaviour factors in the range of 1.5–2.0 is only possible for regions with very low seismicity. This contradicts the observations after recent earthquakes in Italy, where low-rise URM buildings designed to the recent Italian code performed very well, and the results of non-linear static analyses. It is concluded that the results with such low q-factors lead to unrealistically conservative results. This is consistent with the fact that the corresponding mean annual probability of collapse p_{NC} recently found from rigorous probabilistic seismic assessment on code-compliant modern masonry buildings is very low and at least one order of magnitude smaller than the target probability of 2×10^{-4} as proposed in EC8 (CEN 2019a).

This paper focuses on the derivation of rationally based values for the behaviour factor q to be used in linear analyses. The behaviour factor q is subdivided into the components q^*, that accounts for the deformation and energy dissipation capacity, and into the overstrength component *OSR*, that accounts for the redistribution of forces. The introduction of the overstrength ratio *OSR* in the definition of the q-factor for masonry buildings was firstly employed in the Italian Norms but it is a novel aspect within the EC8 framework.

Based on a statistical evaluation of comprehensive pushover analyses results of representative Italian and German URM buildings with "flexural coupled" and "flexural uncoupled" walls, the 5th, 10th, and 50th percentiles of q*, *OSR* and q are derived. Results are given for ultimate shear deformation capacities of 0.20, 0.25, 0.30 and 0.40%, since shear failures govern the global seismic response of the considered buildings. Although the building configurations, modelling approaches and procedures for the calculation of q* of the two studies are quite different, similar values for q*, *OSR*

and q have been obtained. The authors recommend the use of the 10th-fractile for design purposes, which provides, for "flexural coupled" buildings, values of q^* between 1.35 and 1.70, as a function of the maximum shear deformations (range 0.20–0.40%), of *OSR* of 1.50–1.60 and of q between 2.40 and 2.90. In the case of building configurations that can exploit a full redistribution of the forces, the values of q-factors can be taken as the provided overall q-values, independently by the single contributions of q^* and *OSR*. In order to apply the redistribution of the forces and to avoid reduced deformation capacities, the presence of a sufficient number of walls with relatively low axial load ratios σ_0/f_k (e.g., lower than 20% in the seismic design situation) is required, as also incorporated in the new draft of Eurocode 8 and fulfilled in the considered buildings. On the other hand, in the case of configurations where the redistribution of the forces is not possible or it is limited, it is only feasible to use the value of q^*, multiplied by a reduced value of *OSR*. Code-makers can take advantage by the outcomes of this study for the choice of proper values of q^* and *OS*R to be included in standards and codes, possibly as a function of different masonry and structural typologies, once the evaluation of shear drift capacity of walls at ultimate limit state is defined. Such enhanced overall values of q may be consistently included in the codes, as EC8, in relation to other structural systems (as the reinforced masonry/concrete constructions), since the basic component (q^*) remains substantially the same recommended in the current version of EC8 (around 1.50), whereas the increase is mainly due to the introduction of the overstrength contribution for masonry buildings, which is usually larger than that on reinforced constructions.

In addition, the behaviour factor component q_S may be considered to account for overstrength due to the effect of material strength reduction from mean to design values, the possible underestimation of resistances using analytical design approaches in the codes and simplified modelling aspects. The authors believe that, for the factor q_S, values in the range of 1.3–1.5 are reasonable. This component can be applied to further enhance the q-factor value, hence to increase the values of q^* in case of structural configurations unable to exploit the overstrength due to the redistribution of the forces or to raise the overall values of q in case of buildings able to include the contribution of the *OSR*.

The proposed values of q will allow a successful and safe verification of low-rise masonry buildings with proper seismic design and detailing in regions with low and moderate seismicity. Moreover, in redundant structures where redistribution is possible, the application of an effective method for the redistribution of internal forces after linear elastic analyses is also possible; in this regard, further work on this method is currently ongoing. This will lead to design solutions that are more in line with the observations after recent earthquakes and with the results of non-linear analyses.

Although some studies on probabilistic seismic assessment on code-compliant modern masonry buildings designed with q-factors ranging between 2.8 and 3.6 were carried out, showing large safety margins against collapse, a systematic study that correlates the seismic risk to the values of q-factors is still needed to quantify the actual risk levels, for example resorting a method as the one discussed in Fajfar (2018).

Acknowledgements The study presented in the paper was carried out within the research activities of the 2019–2021 ReLUIS Project—WP10 "Code contributions relating to masonry structures", funded by the Italian Department of Civil Protection. The study on the German configurations was financially supported by the German Institute for Structural Engineering (Deutsches Institut für Bautechnik—DIBt).

Authors' contributions PM: conceptualization, methodology, analysis, writing–original draft preparation, writing–review and editing, supervision; CB: conceptualization, methodology, analysis, writing–original

draft preparation, writing–review and editing, funding acquisition; KB: conceptualization, methodology, writing–review and editing, funding acquisition; GM: conceptualization, methodology, writing–review and editing, funding acquisition, supervision. All authors read and approved the final manuscript.

Funding This research activity did not receive any grant from funding agencies in the public, commercial or not-for-profit sectors that may gain or lose financially through publication of this work.

Declarations

Conflict of interest The authors declare that they have no known competing financial interests or personal relationships that could have appeared to influence the work reported in this paper.

References

Allen C, Masia MJ, Derakhshan H, Griffith MC, Dizhur D, Ingham JM (2013) What ductility value should be used when assessing unreinforced masonry buildings?, NZSEE Conference

ASCE-FEMA 356 (2000) Prestandard and Commentary for the Seismic Rehabilitation of Buildings. American Society of Civil Engineers.

Augenti N, Parisi F (2010) Learning from construction failures due to the 2009 L'Aquila, Italy, earthquake. J Perform Constr Facil 24(6):536–555. https://doi.org/10.1061/(asce)cf.1943-5509.0000122

Benedetti D, Carydis P, Pezzoli P (1998) Shaking table tests on 24 simple masonry buildings. Earthquake Eng Struct Dyn 27:67–90

Benedetti D, Castoldi A (1982) "Dynamic and static experimental analysis of stone masonry buildings". Proceedings 7th European Conference on Earthquake Engineering", Athens

Benedetti D (2004) Costruzioni in muratura: duttilità, norme ed esperienze, Ingegneria Sismica, n. 3, 5–18 [in Italian]

Butenweg C, Rosin J, Boesen N (2018) Probabilistic analyses. Research Project: Seismic performance of modern masonry buildings during Emilia 2012 earthquake. Work package 3b-2: Safety margin assessment, SDA-engineering GmbH, Aachen, Germany

Butenweg C, Rosin J, Kubalski T (2019) DIBt-Reports 1 - 4: ISEDEM: Improved seismic design concepts for masonry buildings in Germany/Verbesserte seismische Nachweiskonzepte für Mauerwerksbauten in Deutschland, DIBt-Forschungsvorhaben Nr. P 52–5–3.117–1486/16, SDA-engineering GmbH, Herzogenrath

Butenweg C, Gellert C, Meyer U (2020) Erdbebenbemessung bei Mauerwerksbauten, Mauerwerk Kalender 2020, Verlag Ernst & Sohn

Butenweg C (2013) DGEB Erkundungsreise vom 01.06 – 04.06.2012: Erdbebenschäden in der Emilia Romagna, Norditalien/Earthquake damages in the Emilia Romagna region in North-Italy, DGEB- Publikation No. 15, German Association of Earthquake Engineering and Structural Dynamics

Caliò I, Marletta M, Pantò B (2012) A new discrete element model for the evaluation of the seismic behaviour of unreinforced masonry buildings. Eng Struct 40:327–338

Cattari S, Calderoni B, Caliò I, Camata G, de Miranda S, Magenes G, Milani G, Saetta A (2021) "Nonlinear modelling of the seismic response of masonry structures: critical aspects in engineering practice. Bull Earthq Eng 25:87

Cattari S, Camilletti D, Lagomarsino S, Bracchi S, Rota M, Penna A (2018) "Masonry Italian code-conforming buildings. part 2: nonlinear modelling and time-history analysis", Journal of Earthquake Engineering, Issue sup2: RINTC project: The Implicit Seismic Risk of Italian Code-conforming Structures. Taylor and Francis, Vol. 22, sup2, 2010–2040

CEN (2005b) - EN 1996–1–1, Eurocode 6: Design of masonry structures. Part 1–1: General rules for reinforced and unreinforced masonry structures, 2005b.

CEN (2019a) EN1998–1–1 SC8 25–08–2019a. Eurocode 8: Design of structures for earthquake resistance - Part 1–1: General rules and seismic action, 2019a.

CEN (2019b) Final Draft EN1998–1–2 NEN SC8 PT2 2019b–11–08. Eurocode 8: Design of structures for earthquake resistance - Part 1–2: Rules for new buildings, 2019b.

CEN (1995) Eurocode 8 - Design provisions for earthquake resistance of structures - Part 1-3: General rules - Specific rules for various materials and elements, ENV 1998-1-3:1995, Brussels, Belgium.

CEN (2002) - EN 1990, Eurocode 0: Basis of structural analysis. European Committee for Standardisation, Brussels, Belgium.

CEN (2005a) - EN 1998–1, Eurocode 8: Design of structures for earthquake resistance, Part 1: General rules, seismic actions and rules for building", European Committee for Standardisation, Brussels, Belgium.
DIN EN 1991-1-3/NA, (2010) National Annex – Nationally determined parameter – Eurocode 1: Actions on structures – Part 1-3: General actions – Snow loads. Deutsches Institut für Normung e.V., Berlin
DIN EN 1996–1–1/NA (2012)Nationaler Anhang – National festgelegte Parameter – Eurocode 6: Bemessung und Konstruktion von Mauerwerksbauten – Teil 1–1: Allgemeine Regeln für bewehrtes und unbewehrtes Mauerwerk
DIN EN 1998–1/NA (2020) Nationaler Anhang – National festgelegte Parameter, Eurocode 8: Auslegung von Bauwerken gegen Erdbeben – Teil 1: Grundlagen, Erdbebeneinwirkungen und Regeln für Hochbauten. Deutsches Institut für Normung (DIN), Gelbdruck, Berlin
Dwairi H, Kowalsky M, Nau JM (2007) Equivalent damping in support of direct displacement based seismic design. J Earthq Eng 11:512–530
Fajfar P (1999) Capacity spectrum method based on inelastic demand spectra. Earthq Eng Struct Dyn 28:979–993
Fajfar P (2018) Analysis in seismic provisions for buildings: past, present and future. Bull Earthq Eng 16:2567–2608. https://doi.org/10.1007/s10518-017-0290-8
Fasching S, Jäger A, Gams M (2020) Zyklische Schubversuche an Wänden aus Hochlochziegelmauerwerk Mauerwerk 24 (2020), Heft 3. https://doi.org/10.1002/dama.202000002 [in German]
Fehling E, Stürz J (2007) University of Kassel: Enhanced Safety and Efficient Construction of Masonry Structures in Europe. D 7.1a Test results on the behaviour of masonry under static (monotonic and cyclic) in plane lateral loads
Fehling E, Stürz J, Aldoghaim E (2004) University of Kassel: Enhanced Safety and Efficient Construction of Masonry Structures in Europe. D 7.3 Identification of suitable behaviour factors for masonry members under earthquake loads
Franchin P, Ragni L, Rota M, Zona A (2018) Modelling Uncertainties of italian code- conforming structures for the purpose of seismic response analysis, issue sup2: RINTC project: the implicit seismic risk of Italian code-conforming structures. J Earthq Eng 22(sup2):1964–1989
Freeman SA (1998) The capacity spectrum method as a tool for seismic design, Proceedings of the 11th European Conference on Earthquake Engineering
Frumento S, Magenes G, Morandi P, Calvi GM (2009) "Interpretation of experimental shear tests on clay brick masonry walls and evaluation of q-factors for seismic design", research report EUCENTRE 2009/02. IUSS Press
Giardini D, Woessner J, Danciu L (2014) Mapping Europe's Seismic Hazard. *SHARE Project*. EOS 2014, 95(29):261–262. DOI: https://doi.org/10.1002/2014EO290001. Available on URL: www.share-eu.org
GNDT-CNR (1985). Proposta di nuova normativa sismica. *Ingegneria Sismica* n.1/85, Inserto [in Italian]
Gruppo Sismica. 3DMACRO program (2022) http://www.murature.com/sismica/software.php?id=1
Guerrini G, Graziotti F, Penna A, Magenes G (2017) Improved evaluation of inelastic displacement demands for short-period structures. Earthq Eng Struct Dyn 46(9):1411–1430
Iervolino I, Spillatura A, Bazzurro P (2018) "Seismic Reliability of code-conforming Italian buildings", issue sup2: RINTC project: the implicit seismic risk of Italian code-conforming structures. J Earthq Eng 22(sup2):5–27
Kallioras S, Morandi P, Penna A, Magenes G, (2018a) "Seismic performance assessment of three modern masonry buildings struck by the 2012 Emilia earthquake", Proceedings of the 10th International Masonry Conference, July 9–11 2018a, Milano, Italy
Kallioras S, Morandi P, Magenes G, (2018b) "Results of non-linear probabilistic analysis" Report 3b-1: safety margin assessment; DGFM project - Seismic performance of modern masonry buildings during Emilia 2012 Earthquake
Lagomarsino S, Penna A, Galasco A, Cattari S (2013) TREMURI program: an equivalent frame model for the nonlinear seismic analysis of masonry buildings. Eng Struct 56:1787–1799
Lagomarsino S, Marino S, Cattari S (2020) Linear static procedures for the seismic assessment of masonry buildings: open issues in the new generation of European Codes. Structures 26(2020):427–440. https://doi.org/10.1016/j.istruc.2020.04.003
Lutman M (2018) Slovenian national building and civil engineering institute: seismic response of masonry walls by experimental testing. Report P 577/18–610–1, P 455/17–610–1, P 455/17–610–2, Ljubljana
Lutman M (2019) Slovenian national building and civil engineering institute: seismic response of masonry walls by experimental testing. Report No. 160/19–610–1, Ljubljana
Lutman M (2020) Report No. 515/20–610–1, Seismic response of a masonry wall by experimental testing, Slovenian national building and civil engineering institute, Client: RWTH Aachen University, Center for Wind and Earthquake Engineering

Magenes G, Calvi M (1997) In-plane seismic response of brick masonry walls. Earthq Eng Struct Dyn 26:1091–1112

Magenes G, Manzini C, Morandi P, Remino M, Bolognini D (2006) SAM II Software for the simplified seismic analysis of masonry buildings. University of Pavia and EUCENTRE

Magenes G, Morandi P (2008) "Some issues on seismic design and assessment of masonry buildings based on linear elastic analysis", Proceedings of the Michael John Nigel Priestley Symposium, IUSS Press, Pavia, Italy, July 2008, pp. 83–94. ISBN: 978–88–6198–022

Magenes G, Morandi P, Penna A (2008) "Experimental in-plane cyclic response of masonry walls with clay units", Proceedings of the 14th World Conference *on Earthquake Engineering*, October 12–17 2008, Beijing, China, Paper ID: 12–03–0095

Magenes G Masonry building design in seismic areas: recent experiences and prospects from a European standpoint, Keynote 9, 1st European Conference on Earthquake Engineering and Engineering Seismology, 3–8 september 2006, Geneva, Switzerland, CD-ROM, 2006

Manzini CF, Magenes G, Penna A, da Porto F, Camilletti D, Cattari S and Lagomarsino S (2018) "Masonry Italian Code-Conforming Buildings. Part 1: Case Studies and Design Methods", Journal of Earthquake Engineering, Issue sup2: RINTC project: The Implicit Seismic Risk of Italian Code-conforming Structures. Taylor and Francis, Vol. 22, sup2, 54–73

Meskouris K, Butenweg C, Hinzen K-G, Höffer R (2019) Structural dynamics with applications in earthquake and wind engineering. Springer Verlag

MINEA, Software tool for the design of masonry structures, SDA-engineering GmbH, Kohlscheid, http://www.minea-design.de, 2022

Mistler M, Butenweg C, Fehling E, Stürz J (2007) Verformungsbasierte seismische Bemessung von Mauerwerksbauten auf Grundlage zyklischer Schubwandversuche. Bauingenieur, DACH-Heft, S. 1–11, März

Morandi P, Manzini CF (2020) Magenes G (2020) Application of seismic design procedures on three modern URM buildings struck by the 2012 Emilia earthquakes inconsistencies and improvement proposals in the European codes. Bull Earthq Eng 18:547–580. https://doi.org/10.1007/s10518-019-00650-z

Morandi P, Albanesi L, Graziotti F, Li Piani T, Penna A, Magenes G (2018) Development of a dataset on the in-plane experimental response of URM piers with bricks and blocks. Constr Build Mater 190(2018):593–611. https://doi.org/10.1016/j.conbuildmat.2018.09.070

Morandi P, Albanesi L, Magenes G (2019) In-plane cyclic response of new urm systems with thin web and shell clay units. J Earthquake Eng 25(8):1533–1564. https://doi.org/10.1080/13632469.2019.1586801

Morandi P (2006) New Proposals for simplified seismic design of masonry buildings, PhD Thesis, Rose School, University of Pavia, 2006

Norda H (2012) Beitrag zum statischen nichtlinearen Erdbebenbachweis von unbewehrten Mauerwerksbauten unter Berücksichtigung einer und höherer Modalformen, Dissertation, RWTH Aachen University, Aachen

NTC2008, (2008), "Decreto Ministeriale 14 Gennaio 2008: Norme tecniche per le costruzioni", S.O. No. 30 alla G.U. del 4 Febbraio 2008, No. 29, Ministero delle Infrastrutture e dei Trasporti, Rome, Italy [in Italian]

NTC2018, (2018), "Decreto Ministeriale 17 Gennaio 2018: Aggiornamento delle «Norme tecniche per le costruzioni»", S.O. No. 8 alla G.U. del 20 Febbraio 2018, No. 42, Ministero delle Infrastrutture e dei Trasporti, Rome, Italy [in Italian]

NZS 4230 (User's guide to): Design of Reinforced Concrete Masonry Structures, (2004), *Standard Council New Zealand*, Wellington, New Zealand

OPCM n. 3274. Primi elementi in materia di criteri generali per la classificazione sismica del territorio nazionale e di normative tecniche per le costruzioni in zona sismica, Suppl. ord. n.72 alla G.U. n. 105 del 8/5/2003 [in Italian].

OPCM. n. 3431. Ulteriori modifiche ed integrazioni all'Ordinanza n.3274 del 20/3/2003, recante 'Primi elementi in materia di criteri generali per la classificazione sismica del territorio nazionale e di normative tecniche per le costruzioni in zona sismica' S.O. n.85, G.U. n.107 del 10/5/2005 [in Italian].

Penna A, Morandi P, Rota M et al (2014) Performance of masonry buildings during the Emilia 2012 earthquake. Bull Earthq Eng 12:2255–2273. https://doi.org/10.1007/s10518-013-9496-6

Petry S, Beyer K (2014) Influence of boundary conditions and size effect on the drift capacity of URM walls. Eng Struct 65(2014):76–88

Priestley MJN, Grant DN (2005) Viscous damping in seismic design and analysis. J Earthq Eng 9(229):255

Rosin J, Butenweg C, Cacciatore P, Boesen N (2018) Investigation of the seismic performance of modern masonry buildings during the Emilia Romagna earthquake series. Mauerwerk 22:238–250

2Si. *Pro_SAM* Program (2022). https://www.2si.it/en/pro_sam_eng/.

Sorrentino L, Cattari S, da Porto F, Magenes G, Penna A (2019) (2019): Seismic behaviour of ordinary masonry buildings during the 2016 central Italy earthquakes. Bull Earthq Eng 17(10):5583–5607

STADATA. 3Muri program (2022). https://www.3muri.com
Tomaževič M (1999) Earthquake-resistant design of masonry buildings. Innov Struct Constr 1:87
Tomaževič M, Weiss P (1994) Seismic behaviour of plain and reinforced masonry buildings. J Struct Eng ASCE 120(2):323–338
Tomaževič M, Bosiljkov V and Weiss P (2004) Structural behaviour factor for masonry structures, 13th World Conference on Earthquake Engineering, Vancouver B.C., Canada, paper no. 2642